

**Segmentation of Retinal Vasculature using Active Contour Models (Snakes)**

by

Pang Kee Yong

Dissertation submitted in partial fulfilment of  
the requirements for the  
Bachelor of Engineering (Hons)  
(Electrical & Electronic Engineering)

JUNE 2009

Universiti Teknologi PETRONAS  
Bandar Seri Iskandar  
31750 Tronoh  
Perak Darul Ridzuan

# **CERTIFICATION OF APPROVAL**

**Segmentation of Retinal Vasculature using Active Contour Models (Snakes)**

by

Pang Kee Yong

A project dissertation submitted to the  
Electrical & Electronics Engineering Programme  
Universiti Teknologi PETRONAS  
in partial fulfilment of the requirement for the  
BACHELOR OF ENGINEERING (Hons)  
(ELECTRICAL & ELECTRONICS ENGINEERING)

Approved by,



---

(Mrs. Lila Iznita binti Izhar)  
Project Supervisor

UNIVERSITI TEKNOLOGI PETRONAS

TRONOH, PERAK

JUNE 2009

## **CERTIFICATION OF ORIGINALITY**

This is to certify that I am responsible for the work submitted in this project, that the original work is my own except as specified in the references and acknowledgements, and that the original work contained herein have not been undertaken or done by unspecified sources or persons.



---

(PANG KEE YONG)

## ABSTRACT

Characteristic of retinal vasculature has been an important indicator for many diseases such as hypertension and diabetes. A digital image analysis system can assist medical experts to make accurate diagnosis in an efficient manner. This project presents the computer based approach to the automated segmentation of blood vessels in retinal images. The detection of the retinal vessel is achieved by performing image enhancement using CLAHE followed by Bottom-hat morphological transformation. Active contour model (snake) that based on level sets, techniques of curve evolution, and Mumford-Shah functional for segmentation is then used to segment out the detected retinal vessel and produce a complete retinal vasculature. A Graphic User Interface (GUI) has also been created to ease the user for the segmentation of the retinal vasculature. The algorithm is then tested with 20 test images from the DRIVE database. The results shows that the algorithm outperforms many other published methods and achieved an accuracy (ability to detect both vessel and non-vessel pixels) range of 0.92-0.94, a sensitivity (ability to detect vessel pixels) range of 0.91-0.95 and a specificity (ability to detect non-vessel pixels) range of 0.78-0.85.

## ACKNOWLEDGEMENT

First and foremost, I would like to render my appreciative gratitude to Mrs. Lila Iznita Izhar, the supervisor for this project, for all her invaluable help, advices, suggestions, and encouragement given while doing the project, right from its conception to its completion. Her untiring effort has been a continuous inspiration to me.

I would like to express my gratitude and thanks to Dr. Vjanth, Mr. Hanung, and Mr. Hermawan. The project would have taken a much longer time or not even have been completed without their advice, suggestions, and continuous help. Their help in giving ideas image processing techniques for retinal images are one of the key factors of the success of this project.

I would like to gratefully acknowledge the Electrical and Electronics Engineering Department for providing resources, facilities, and needs during this research. My whole hearted thanks to my colleagues for their constructive comments and knowledge sharing during the progress of this project. I would also like to express my appreciation to my parents for their loving support and encouragement in so many ways. Lastly, I wish to thank all those who were involved either directly or indirectly for their help in completing this project.

## TABLE OF CONTENTS

<b>ABSTRACT</b> .....	<b>iv</b>
<b>ACKNOWLEDGEMENT</b> .....	<b>v</b>
<b>LIST OF FIGURES</b> .....	<b>viii</b>
<b>LIST OF TABLES</b> .....	<b>x</b>
<b>CHAPTER 1 INTRODUCTION</b> .....	<b>1</b>
1.1 Background of Study .....	1
1.2 Problem Statement .....	1
1.3 Objectives.....	1
1.4 Scope of Study .....	1
<b>CHAPTER 2 LITERATURE REVIEW</b> .....	<b>2</b>
2.1 Medical Knowledge .....	2
2.2 Medical Imaging .....	6
2.3 Image Pre-processing Techniques .....	7
2.4 Image Segmentation for Medical Imaging.....	15
2.5 Analysis Method for Retinal Image .....	29
<b>CHAPTER 3 METHODOLOGY</b> .....	<b>31</b>
3.1 Project Methodology.....	31
3.2 Vessel Detection Phase .....	32
3.3 Vessel Segmentation Phase.....	35
3.4 Performance Analysis of Detection and Segmentation of Retinal Vasculature....	37
3.5 Tools.....	39
3.6 Key Milestones .....	39

<b>CHAPTER 4 RESULTS AND DISCUSSION.....</b>	<b>40</b>
4.1 Results .....	40
4.2 Discussion.....	50
<b>CHAPTER 5 CONCLUSION AND RECOMMENDATION.....</b>	<b>52</b>
5.1 Conclusion.....	52
5.2 Recommendation.....	52
<b>REFERENCES.....</b>	<b>53</b>
<b>APPENDICES.....</b>	<b>59</b>
Appendix A1: Gantt Chart for the Final Year Project (1 <sup>st</sup> Semester)	
Appendix A2: Gantt Chart for the Final Year Project (2 <sup>nd</sup> Semester)	
Appendix B : Information of the Fundus Camera.	
Appendix C : Images from DRIVE Database	
Appendix D : Project Source Codes	

## LIST OF FIGURES

Figure 1 Mechanism of Hypertension .....	2
Figure 2 Retinal .....	4
Figure 3 Hypertensive Retinopathy's Sign .....	5
Figure 4 Example of hypertensive Retinopathy Fundus Image.....	6
Figure 5 Non Mydratic Fundus Camera .....	7
Figure 6 Colour Retinal Image .....	7
Figure 7 RGB Colour Coordinate.....	7
Figure 8 Colour channel for the retinal image.....	8
Figure 9 Bilinear Intertolation .....	9
Figure 10 Bi-cubic Interpolation .....	10
Figure 11 Image Interpolation .....	10
Figure 12 Mean Filtering.....	11
Figure 13 Median Filtering.....	12
Figure 14 Original Image and Histogram.....	13
Figure 15 Image and Histogram after Contrast Stretching.....	13
Figure 16 Image and Histogram after Histogram Equalization.....	13
Figure 17 Histogram after Histogram Equalization.....	14
Figure 18 CLAHE process.....	15
Figure 19 Image and Hitogram after CLAHE .....	15
Figure 20 Example of detected centrelines.....	16
Figure 21 Retion Growing .....	17
Figure 22 Morphology Operation by binary image .....	19
Figure 23 Morphology Operation by gray scale imagev .....	20
Figure 24 Morphological Operation .....	21
Figure 25 Active Contour Model.....	22
Figure 26 Demo of Snake Opetations.....	23
Figure 27 Segmentation results for water flow method.....	25
Figure 28 Result for an ultrasound image of carotid artery using Level Set Method .....	27

Figure 29 Retinal Exudates .....	29
Figure 30 Bifurcation angle .....	29
Figure 31 Size of optic disc for hypertensive and diabetic .....	30
Figure 32 arterial and veinal diameter measurement .....	30
Figure 33 Tortuous for hypertensive and diabetic .....	30
Figure 34 Design Proces .....	31
Figure 35 Vessel Detection Phase.....	32
Figure 36 Reference Fundus Image (TIF Format) .....	32
Figure 37 Linear structuring element.....	34
Figure 39 Initial Contour.....	36
Figure 38 Conditions for the Energy Function .....	36
Figure 40 Colour channel for TIF format .....	40
Figure 41 TIF Image for Median Filtering.....	41
Figure 42 TIF Image for contrast enhancement.....	41
Figure 43 TIF Image after morphological operation.....	42
Figure 44 TIF Image after background removal process .....	43
Figure 45 Results of Active Contour Model.....	44
Figure 46 Segmentation of one image from DRIVE database.....	46
Figure 47 Segmentation of one image from DRIVE database.....	47
Figure 48 Development of Graphic User Interface.....	48
Figure 49 Layout of the GUI.....	49

## **LIST OF TABLES**

Table 1	Classifications of blood pressure.....	3
Table 2	Stage of Hypertensive Retinopathy (Keith-Wagener classification).....	6
Table 3	Tool Needed for the Project.....	39
Table 4	Performance parameters (based on 20 test images from DRIVE database).....	45
Table 5	Accuracy achieved by the published methods reproduced from [50] .....	46

# CHAPTER 1

## INTRODUCTION

### 1.1 Background of Study

Hypertension and diabetes are common diseases in the world as well as Malaysia. Statistics shows that more than 32 percent or an estimated 2.6 million Malaysian adult aged 30 or above have hypertension [1]. Among these hypertensives in Malaysia, only 33% are aware of their hypertension [1]. On the other hand, the diabetic population in Malaysia has also increased over four-fold from 300,000 in 1996 to 1,383,675 in 2005 [2] [3].

In addition to this, prolonged hypertension and diabetes without any treatment will cause damages to our body organs or even cause mortality. For example, prolonged hypertension will cause stroke or heart failure while prolonged diabetes will caused blindness. As a result, early detection of these diseases is very important and an accurate method for diagnosis is needed.

The retinal blood vessel appearances are landmarks for many diagnoses, including hypertension, diabetes, arteriosclerosis, cardiovascular disease, and stroke [4]. For these diagnoses, measurements are needed such as vessel width, colour, tortuosity, reflectivity, or abnormal branching. A tool that could perform diagnosis of these diseases based on accurate and objective analysis of symptoms at their early stage is very important to cater for early and effective treatment of these diseases. Among the features in ocular fundus image, the structure of retinal vessel plays an important role in revealing these diseases. Hence, the development of an effective and efficient computer based approach to the automated segmentation of blood vessels in retinal images would allow medical experts to screen large numbers of vessel abnormalities.

## **1.2 Problem Statement**

The retinal image has become an important tool in revealing diseases such as diabetes and hypertension. The diagnoses of these diseases relied very much on the structure of the retinal blood vessels. As a result, the accuracy of the segmented retinal vasculature is important to assist future analysis such as analysis of foveal avascular zone [5], tortuosity and etc.

However, detecting blood vessels from a retinal image is a challenging problem due to the width of retinal vessels can vary from very small to very large, the reflection on the tiny uneven surface of the soft tissue in the image, the unstable local contrast of blood vessels, and the pathological variation.

Hence, these problems drive to the focus of this project which is on the development of algorithm to segment a complete vasculature automatically from the colour fundus images with inconsistent contrast using a model based approach, Active Contour Model (Snake).

## **1.3 Objectives**

The main objectives of this project are to design and develop an algorithm to segment retinal vasculature in low and inconsistent contrast colour fundus images and create a Graphic User Interface for the segmentation of retinal vasculature.

## **1.4 Scope of Study**

In general, the project encompasses the following scopes of study:

- Biomedical image processing techniques
- Segmentation methods in medical imaging
- Medical information on diagnoses using retinal images

## CHAPTER 2

### LITERATURE REVIEW

#### 2.1 Medical Knowledge

##### 2.1.1 Hypertension

Hypertension is the medical name for high blood pressure. Blood pressure is the force of blood in the arteries (Please refer to figure 1). When the heart beats, blood propels in the arteries with force. This is called systolic blood pressure. When the heart relaxes after each beat, the force of the blood flow drops (called diastolic blood pressure) [6]. So, in general, hypertension is the chronic state of elevated pressure in the arteries.

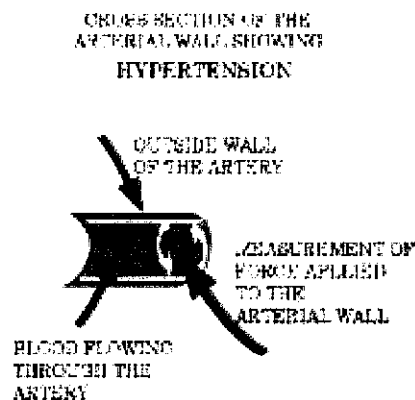


**Figure 1 Mechanism of Hypertension**

(Image Adapted from [75])

Blood pressure readings are always given as two numbers, as the force of your blood pressure is measured in two ways. They are always represented by a fraction for example 120/90; the top pressure (120) is your systolic reading, which is measured just after your heart beats. The bottom pressure (90) is your diastolic pressure measured in between heartbeats, when your heart is relaxed and filling with blood.

A person with systolic and/or diastolic blood pressures consistently above the normal range (120/80 mm Hg) is said to have hypertension [6] Apparently, hypertension can be divided into several stages which indicates the severity of the disease (Please refer to Table 1)

**Table 1 Classifications of blood pressure (Table adapted from [7])**

<b>Classification of Blood Pressure</b>		
	<b>Systolic BP, mm Hg</b>	<b>Diastolic BP, mm Hg</b>
Normal	<120	and <80
Prehypertension	120-139	or 80-89
Stage 1 hypertension	140-159	or 90-99
Stage 2 hypertension	>160	or >100

Hypertension is known as the “silent killer”, as most people do not experience any symptoms [8]. If the disease being unaware for a long term, it will prolonged the stress to the body organs and lead heart failure, hardening of vessels, kidney failure, bleeding and damage to the light-sensitive area of the eyes, and stroke. Besides, rapid rise blood pressure will also cause confusion, drowsiness, fits and even death and must be treated urgently.

Besides measuring the blood pressure using sphygmomanometer, patients with higher-than-normal blood pressure is encouraged to be given other tests. These include:

- Medical and family histories. -If hypertension is common in the family, the patient is likely to be at higher risk for the condition.
- Physical examination. - Sometimes other health problems may be discovered during a physical examination that explains the patient's high blood pressure.
- Examination of the blood vessels in the eyes. - High blood pressure may cause blood vessels in the eyes to become thick or narrow.
- Chest X ray. - This is used to check for an enlarged heart, other heart disorders, and lung disease.
- Electrocardiograph (ECG). - This test measures the electrical activity of the heart.
- Blood and urine tests. - These help determine the general health of the patient.

### 2.1.2 Retinal Blood Vessel

From the theory, the retina has two parts: the peripheral retina and the macula. The macula is like the bull's-eye which is very small while the peripheral retina is the large area of the retina that surrounds the macula and makes up 95% of the retina (Please refer to Figure 2).

If you observe Figure 2 properly, there are dark and curving lines in the retina. These are the blood vessels of the retina. The blood vessels bring oxygen and nutrition to the retina. In order for the peripheral retina and macula to work properly, the blood vessels must be normal.

Retinal vessel is always an indicator of several diseases such as diabetes and hypertension. From the studies, retinal vessel changes are common findings in patients suffering from long-standing hypertensive disease. Morphological evaluations of the fundus oculi represent a fundamental tool for the clinical approach to the patient with hypertension [9]

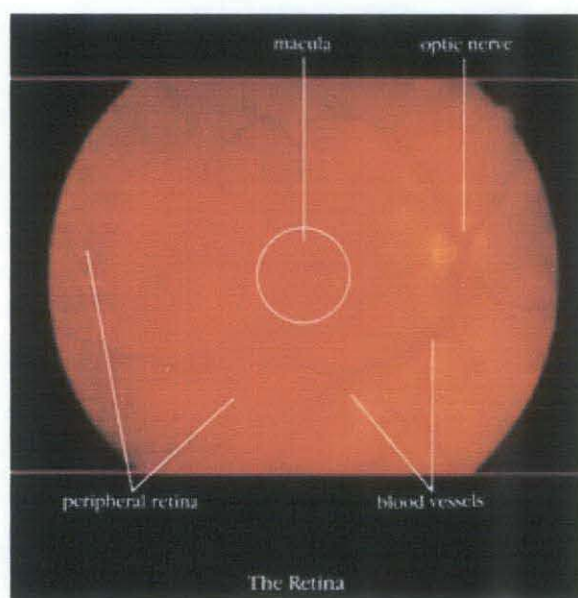


**Figure 2 Retinal**  
(Image Adapted from [10])

### 2.1.3 Hypertensive Retinopathy

Hypertensive retinopathy is damage to the retina due to high blood pressure [11]. The retina is one of the "target organs" that are damaged by several disease especially sustained hypertension. Long-standing hypertension appears to lead to retinal arteriolar narrowing, according to the latest results from the Blue Mountains Eye Study (BMES) [12]. In general, the patient with hypertensive retinopathy, as expected, suffers from hypertension. However, the hypertension may be unknown to the patient and the eye exam may yield the first clue to this relative asymptomatic systemic disease [13].

Some of the first sign in the hypertensive retinopathy are flame hemorrhages and cotton wool spots [13]. As hypertensive retinopathy progresses, hard exudates can appear around the macula along with swelling of the macula and the optic nerve, causing impairment of vision. In severe cases permanent damage to the optic nerve or macula can occur (See Figure 3).

There is one retinal fundus image example for hypertensive retinopathy in Figure.4 The retinal arteries have become narrow and tortuous. In more advanced cases haemorrhages and 'star burst' exudates occur together with papilloedema [14].

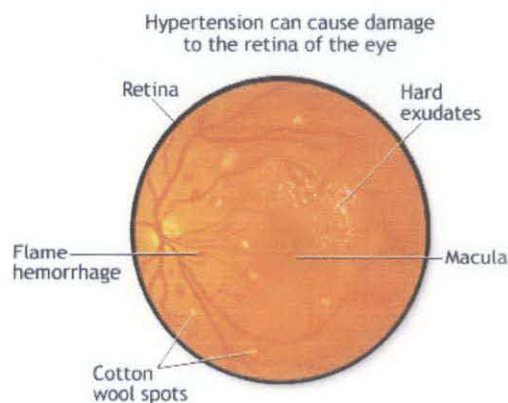


**Figure 3 Hypertensive Retinopathy's Sign**

Image adapted from [11]

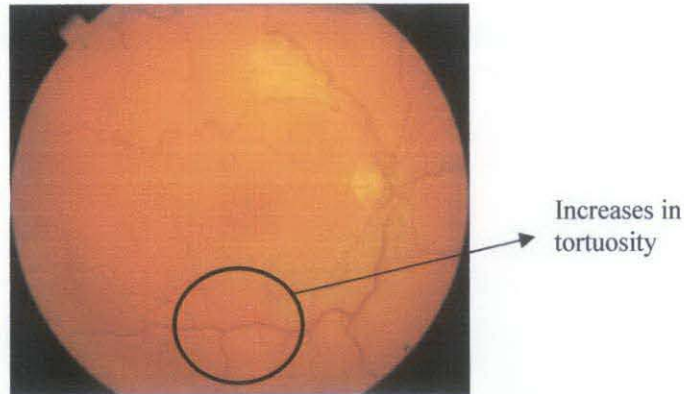


**Figure 4 Example of hypertensive Retinopathy Fundus Image**

(Image Adapted from [14])

From Keith-Wagener classification, hypertensive retinopathy can be divided into 4 stages according to the sign such as cotton wool exudates, flame haemorrhages and etc. The stages of the disease are shown in Table 2.

**Table 2 Stage of Hypertensive Retinopathy (Keith-Wagener classification)**  
(Table adapted from [15])

Stage	Signs
I	Arteriolar narrowing and tortuosity Increased light reflex "Silver wiring"
II	Arteriovenous nipping
III	Cotton-wool "exudates" Flame and blot hemorrhages
IV	Papilledema

## 2.2 Medical Imaging

### 2.2.1 Fundus Imaging

The definition of fundus is the bottom or base of anything. In medicine, it is a general term for the inner lining of a hollow organ [16]. The ocular fundus is the inner lining of the eye made up of the sensory retina, the retinal pigment epithelium, bruch's membrane, and the choroid [16]. When performing ophthalmic fundus photography for diagnostic purposes, the pupil is dilated with eye drops and a special camera called a

fundus camera is used to focus on the fundus. The resulting images can be spectacular, showing the optic nerve through which visual "signals" are transmitted to the brain and the retinal vessels which supply nutrition and oxygen to the tissue set against the red-orange color of the pigment epithelium [16].



**Figure 5 Non Mydratric Fundus Camera**  
(Image Adapted from [65])

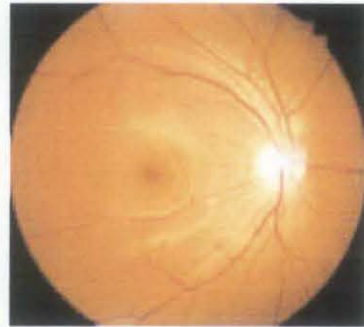


**Figure 6 Colour Retinal Image**  
(Image Adapted from [16])

## 2.3 Image Pre-processing Techniques

### 2.3.1 Image Conversion

Normal colour images are represented in RGB model. In this model, each colour appears in its primary spectral components of red, green and blue. This model is based on a Cartesian coordinate system which shown in Figure7. To simplify the manipulation process, the image can be converted to greyscale or its colour channel as show in the following sub section.

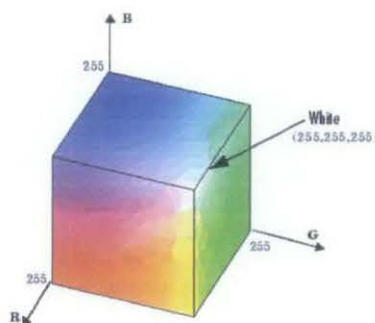


**Figure 7 RGB Colour Coordinate**

Theoretically, red, green and blue filters each will transmit one third of white light while blocking the other two thirds. In general, these filters will lighten their own color while darkening the other two. Figure 8 demonstrates the effect of the three primary color filters on a fundus images.

In this case, blue light is mostly absorbed by the RPE, retinal blood vessels, choroidal blood and the optic nerve. It results a very dark background against which the specular reflections and scattering in the anterior layers of the fundus is enhanced [17]. In addition, for this fundus image, the green channel gives the highest contrast between vessel and background because although green light is also absorbed by blood, but is reflected more by the RPE than blue. There is less scatter than with shorter wavelengths, so media opacities have less of a detrimental effect [17].

On the other hand, the red channel image is too bright compare to the other channels, That is because with red light, the RPE becomes a bit more transparent revealing a better view of the choroidal pattern [17].

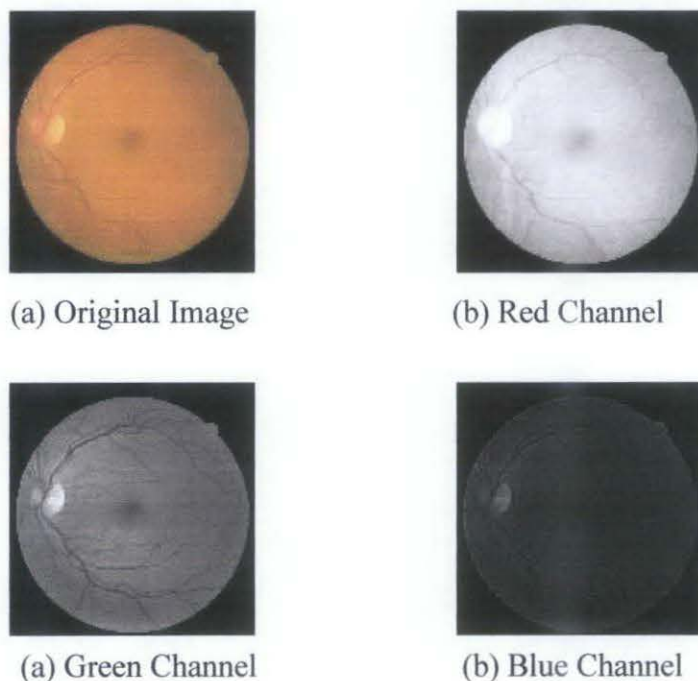


**Figure 8 Colour channel for the retinal image**

### 2.3.2 Image Resizing/Scaling

Image resizing used to magnify or reduce the size of an image. This process is important for digital image processing in manipulating and analyzing the image. There are three sampling methods for scaling process which are nearest-neighbour interpolation method, bilinear interpolation method, and bi-cubic interpolation method.

#### 2.3.2.1 Nearest-neighbour interpolation

Nearest neighbor is the most basic and requires the least processing time of all the interpolation algorithms because the output pixel is assigned the value of the pixel that the point falls within. No other pixels are considered. The position error of the nearest neighborhood interpolation is at most half a pixel.

This error is perceptible on objects with straight line boundaries that may appear step-like after the transformation [18].

#### 2.3.2.2 Bilinear interpolation

Bilinear interpolation considers the closest 2x2 neighbourhood pixel. It then takes a weighted average of these 4 pixels to arrive at its final interpolated value [19]. This results in much smoother looking images than nearest neighbour.

Although the problems of step-like straight boundaries with the nearest neighborhood interpolation is reduced compared to neighbor interpolation, but the linear interpolation still cause a small decrease in resolution and blurring due to its averaging nature [20].

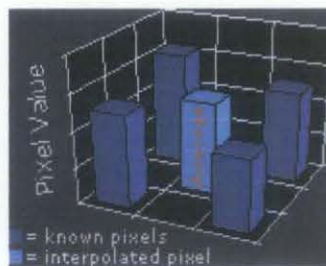


**Figure 9 Bilinear Interpolation**

(Image Adapted [19])

### 2.3.2.3 Bicubic interpolation

Bicubic goes one step beyond bilinear by considering the closest 4x4 neighborhood of known pixels-- for a total of 16 pixels. Since these are at various distances from the unknown pixel, closer pixels are given higher weighting in the calculation (See Figure10).

Bicubic interpolation does not suffer from the step-like boundary problem of nearest neighborhood interpolation, and copes with linear interpolation blurring as well. Bicubic interpolation preserves fine details in the image very well.

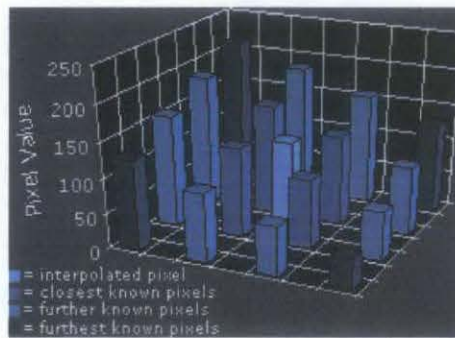


**Figure 10 Bi-cubic Interpolation**  
(Image Adapted from [19])

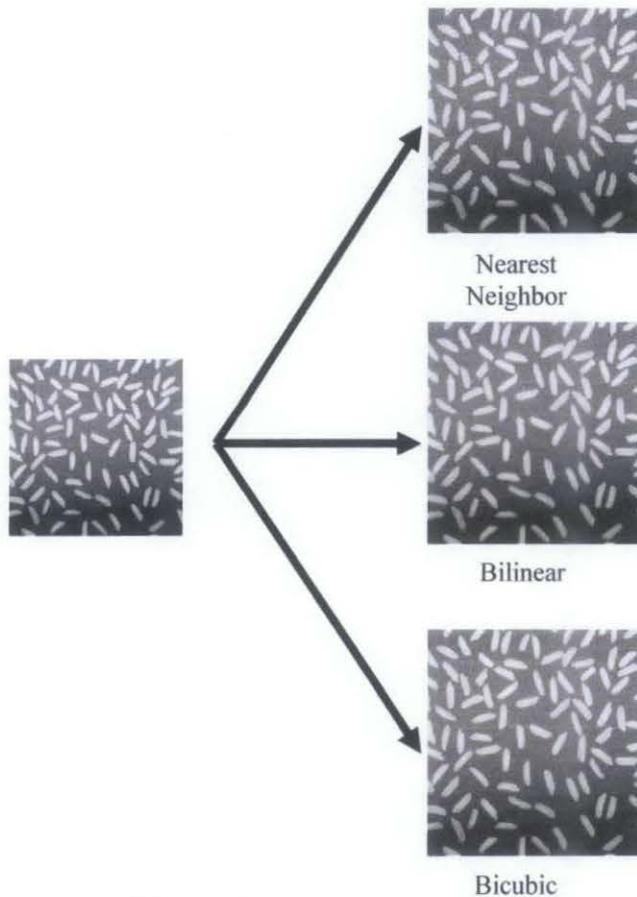


**Figure 11 Image Interpolation**

### 2.3.3 Noise Reduction Methods

Image noise is a random, usually unwanted information in an image. Image noise can originate in film grain, or in electronic noise or in the unavoidable shot noise or an ideal photon detector. Example of image noise are salt and pepper noise, Gaussian noise and shot noise. The main objective of reducing noise is to eliminate unwanted information in an image. To achieved this objective, smoothing filters are used which will be explained in the following sections.

#### 2.3.3.1 Low Pass Filter

Low pass filtering is a process used for smoothing or lowering the noise of an image. Mean filter is the simplest type of low-pass filter and it is used to soften an image by averaging surrounding pixel values. A Simple 3x3 mean rectangular filter is defined by :

$$C = \frac{1}{K} \cdot \begin{bmatrix} 1 & 1 & 1 \\ 1 & 1 & 1 \\ 1 & 1 & 1 \end{bmatrix}; k = 9$$

The smoothing effect depends strongly on the filter kernel size where the larger the kernel, the larger the smoothing effect. With large kernel sizes the smoothed value becomes more dependent on values lying further away from the current position [21]. The choice of kernel size is a compromise between a desired noise reduction and keeping the image sharpness. The serious disadvantage of this filter is the blurring effect as shown in Figure 12.



(a) Original Image



(b) After mean filtering

**Figure 12 Mean Filtering**

### 2.3.3.2 Median Filter

Median filter is quite popular because they effectively reduce certain types of random noise with considerably less blurring than other smoothing filter of similar size [22]. The function of this filter is to replace the intensity value of the center pixel by the median intensity value in its neighbourhood. Its edge-preserving nature makes it useful in cases where edge blurring is undesirable (See Figure13).

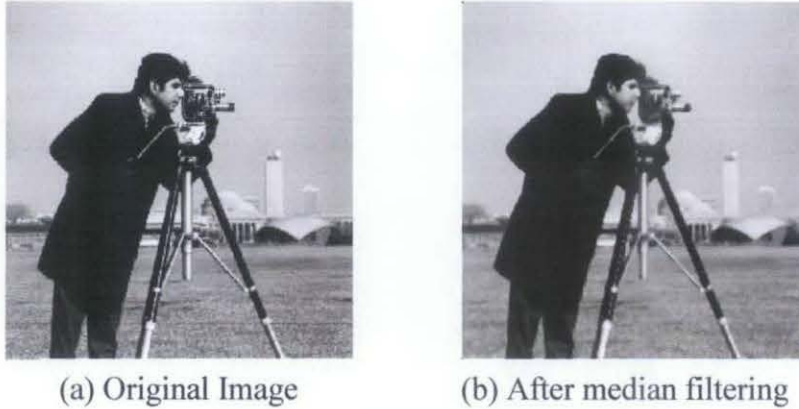


**Figure 13 Median Filtering**

Unfortunately, median filter tends to eliminate thin lines and sharp corners of the image in a rectangular neighbourhood [23]. This problem can be solved by using different shape of neighbourhood or by performing to a magnified version of input image where thin line will be preserved by using these method.

### 2.3.4 Contrast Enhancement

Low contrast images can result from poor illumination, lack of dynamic range in the imaging sensor, or even wrong setting of a lens aperture during image acquisition [22]. To overcome this issue, there are several methods such as contrast stretching and histogram equalization.

#### 2.3.4.1 Contrast Stretching

Contrast stretching is one of the simplest contrast enhancement methods which attempt to improve the contrast in an image by 'stretching' the range of intensity values it contains to span a desired range of values [22].

It differs from the more sophisticated histogram equalization in that it can only apply a linear scaling function to the image pixel values [24]. As a result, the 'enhancement' is less harsh.

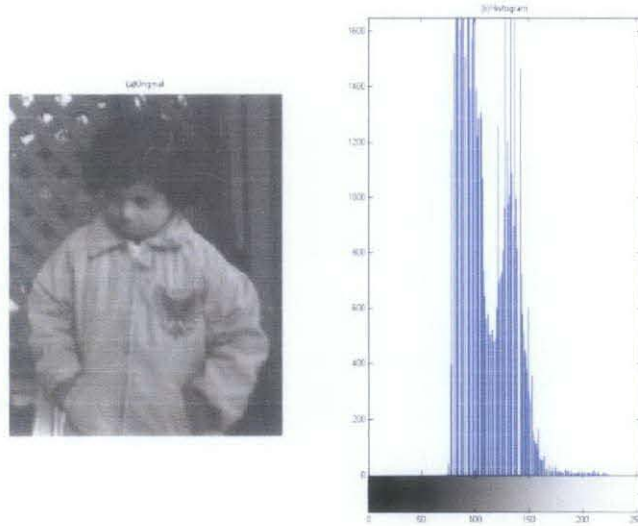


**Figure 14 Original Image and Histogram**

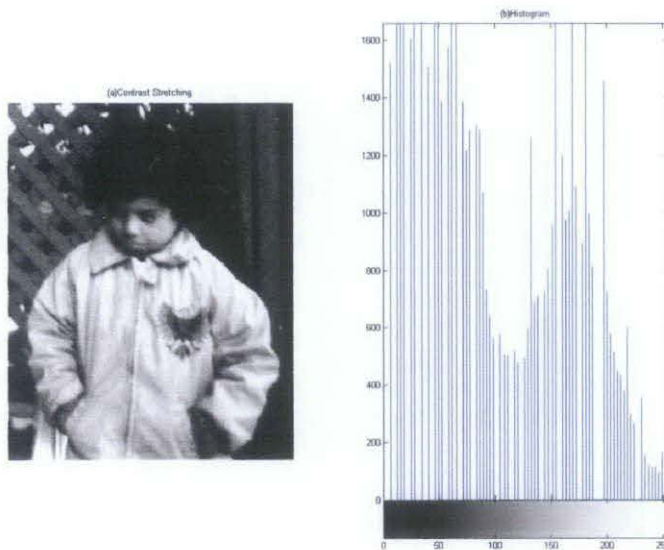


**Figure 15 Image and Histogram after Contrast Stretching**

#### 2.3.4.2 Histogram Equalization

Histogram equalization techniques provide a sophisticated method for modifying the dynamic range and contrast of an image by altering that image such that its intensity histogram has a desired shape. Histogram equalization employs a monotonic, non-linear

mapping which re-assigns the intensity values of pixels in the input image such that the output image contains a uniform distribution of intensities [25].



**Figure 16: Image after Histogram Equalization**

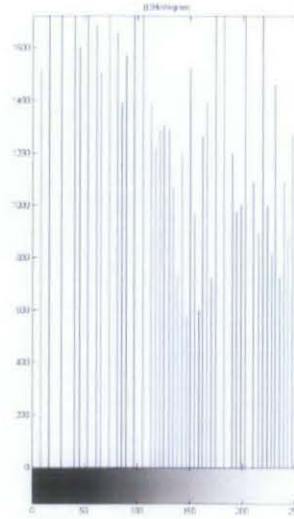


**Figure 17 Histogram after Histogram Equalization**

#### 2.3.4.3 Contrast Limited Adaptive Histogram Equalization (CLAHE)

Some images such as fundus images have many different brightness region such as the optic disc region, macular region and etc. Therefore, global enhancement method such as contrast stretching is not very efficient to enhance completely for the whole retinal vasculature.

Contrast limited adaptive histogram equalization (CLAHE) is a window based enhancement method. Unlike histogram equalization works globally on the entire image, CLAHE operates on small regions in the image, called tiles [26]. Each tile's contrast is enhanced, so that the histogram of the output region approximately matches a specified histogram (See figure18). After performing the equalization, CLAHE will combine all the neighbouring tiles using bilinear interpolation to eliminate artificially induced boundaries.

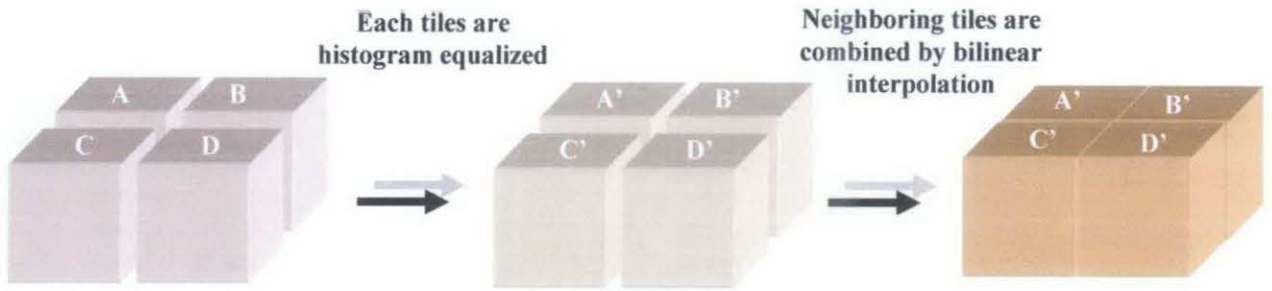


**Figure 18 CLAHE process**

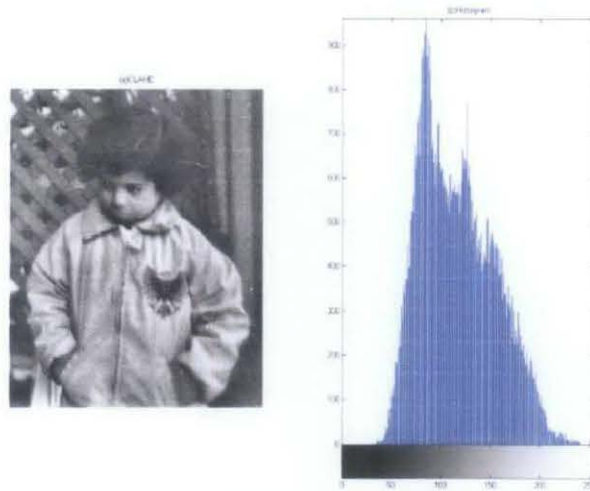


**Figure 19 Image and Hitogram after CLAHE**

## 2.4 Image Segmentation for Medical Imaging

There are many types of approaches for medical image segmentation especially in retinal blood vessel extraction. All the proposed methods have their advantages and disadvantages based on the characteristic of the object of interest and the method of segmentation. From the studies, the segmentation methods can generally be separated into the following 5 categories:

### 2.4.1 Pattern Recognition Approaches

Pattern recognition is used for region and object classification. It is one of the method to object of interest in medical imaging such as blood vessel, ventricles, tumour and etc. In pattern recognition, there are several techniques which shown below:

#### 2.4.1.1 Skeleton based approaches

For this approach, it is commonly used in detecting retinal blood vessel. Vessel centrelines are extracted and then connected to create a vessel tree. In [27], they locating the centrelines using the normalized gradient vector field and also the skeletonization morphological operation. In this research, the final centreline is defined by combining both low contrast and high contrast center line and the artifacts is removed by pruning away the pixel which is far away from the centreline [27].

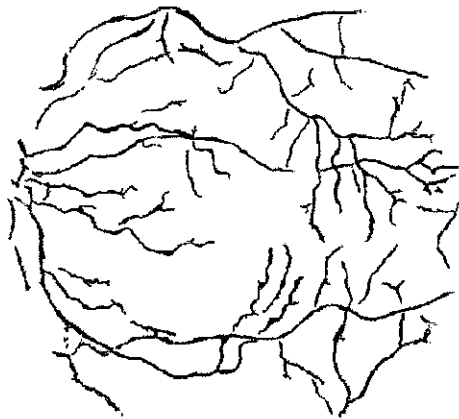


**Figure 20 Example of detected centrelines**

(Image adapted from [27])

#### 2.4.1.2 Ridge-Based approaches

The ridge based approach is a specialized version of skeleton based approach. It has been used to extract retinal blood vessel. This system is focus on extracting the image ridges, which coincide approximately with vessel centreline [28]. The ridges are used to compose primitives in the form of line elements. The sets are used for 2 purposes. First, features are computed which together with a classifier give a probability that the line element is part of the vessel [28]. Second, with the line elements an image is partitioned into patches by assigning each image pixel to the closest line element. Every line element constitutes a local coordinates frame for its corresponding patch. The probability that the line element is part of a vessel is one of the features. The features are used to classify the pixels in the patch into vessel or non-vessel [28]. This method is a type of supervised methods such as neural network. Although ridge based segmentation has good

performance but this technique has a significant disadvantage which it requires manually labelled images for training. For the Utrecht database used by [28], it took an observer 2 hours on average to label a single image.

### 2.4.1.3 Region growing approaches

Region growing is functioned to group pixels or sub-regions into larger regions based on predefined criteria. It can be classified as pixel based image segmentation and the main objective of this process is to find regions of inconsistent contrast levels and edges around them.

The basic approach is to start with a set of seed points and from these grow regions by appending to each seed those neighbouring pixels that have properties similar to the seed [22]. The initial regions are at the exact location of those seeds. Then the regions are grown from these seeds to adjacent points depending on a threshold or criteria we make. It would be gray level texture, or colour. In this region growing process, when the growth of one region stops, another seed pixel which does not yet belong to any region will be chosen and the step will be repeated. This whole process is repeated until all pixels are belonged to some region.

There are three possible ways for a seed pixel to grow which are four side-connectivity, four diagonal-connectivity, and eight connectivity (See Figure 23).

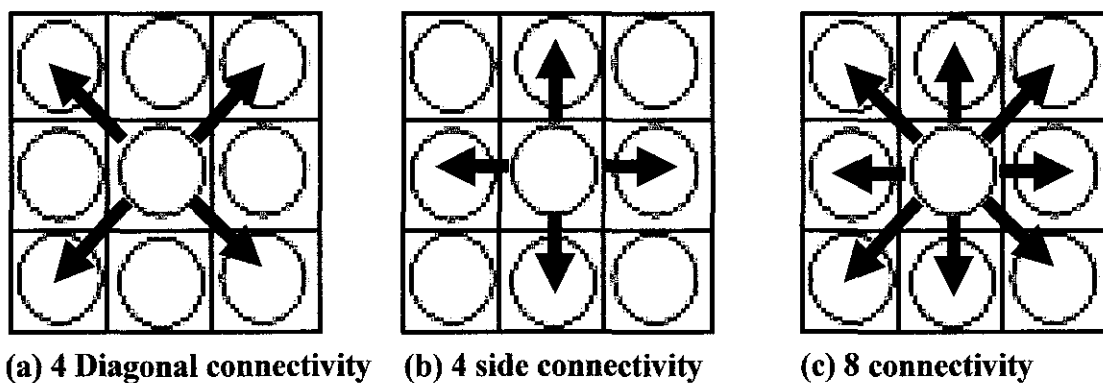


Figure 21 Region Growing

Binary image will be the result of seed based region growing. The extracted region of interest will be the white region and rest will be the black background.

The main disadvantage of this method is the seed point need to be selected manually. The user needs to have at least the basic understanding of image processing in order to place the seed effectively.

#### *2.4.1.4 Matched filter approaches*

Matched filter approaches are signal processing approaches where new images with un-extracted vessels are convolved with known profiles of vessels. A match filter describes the expected appearance of a desired signal, for the purposes of comparative matching [29]. In [30], a Gaussian function is proposed as a model for a blood vessel profile. The model is extended to 2-D by assuming a vessel has a fixed width and direction for a short length. Since vessel may appears in any orientation, a set of 2-D segment profiles in equiangular rotations is used as a filter bank [29]. The filters are implemented using twelve 16x16 pixel kernels. The details for computing the actual values in the kernels may be found in [30]. Matched filters are normally followed by image processing operations like thresholding to get the final vessel contours such as thresholding probing in [30].

#### *2.4.1.5 Morphological Operations*

Morphology is a technique of image processing based on shapes [31]. The value of each pixel in the output image is based on a comparison of the corresponding pixel in the input image with its neighbours. By choosing the size and shape of the neighbourhood, you can construct a morphological operation that is sensitive to specific shapes in the input image. There are several morphological functions such as dilation, erosion, and etc which will discuss in the following sections.

##### *i. Dilation and Erosion*

Dilation and erosion are two fundamental morphological operations. In general, dilation adds pixels to the boundaries of objects in an image while erosion removes pixels on object boundaries. [32]. Thus, for dilation, areas of foreground pixels grow in size while

holes within those regions become smaller while for erosion, areas of foreground pixels shrink in size, and holes within those areas become larger..

These operations can be applied for specific operations by using suitable structuring element. Structuring elements consist of a matrix of 0's and 1's, typically much smaller than the image being processed. The center pixel of the structuring element, called the origin, identifies the pixel of interest which is the pixel being processed. This structuring element will determines the precise effect of the dilation on the input image.

For binary images, with A as an image input image and B as the structuring element, the dilation of A by B and erosion A by B are denoted below and it shows graphically below .

Dilation :  $D(A, B) = A \oplus B = \bigcup_{\beta \in B} (A + \beta)$   
 Erosion :  $E(A, B) = A \ominus B = \bigcap_{\beta \in B} (A - \beta)$

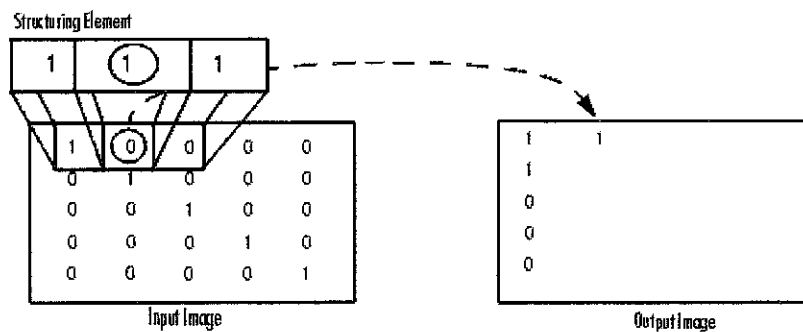


**Figure 22 Morphology Operation by binary image**

(Image adapted from [32])

For gray scale images, with  $f(x,y)$  as input image and  $b(x,y)$  as structuring element, the dilation and erosion are denoted below and its graphical representation are shown in figure 21.

Dilation :

$$(f \oplus b)(s, t) = \max\{f(s - x, t - y) + b(x, y) | (s - x), (t - y) \in D_f; (x, y) \in D_b\}$$

Erosion :

$$(f \otimes b)(s, t) = \min\{f(s + x, t + y) - b(x, y) | (s + x), (t + y) \in D_f; (x, y) \in D_b\}$$

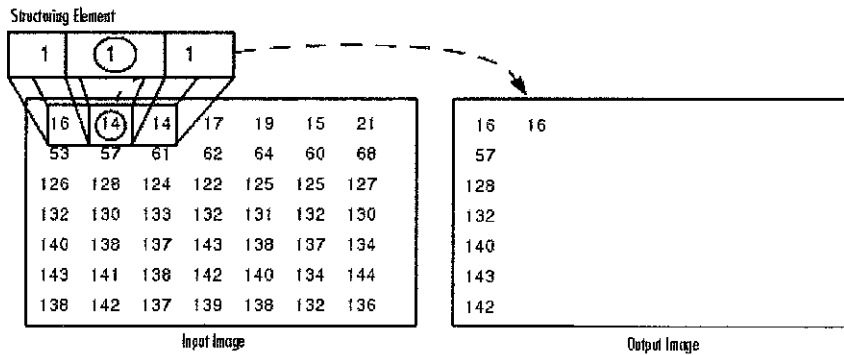


**Figure 23 Morphology Operation by gray scale imagev**

(Image adapted from [32])

ii. *Opening and Closing*

Opening is an important mathematical morphology operation. It is derived from fundamental morphology operation dilation and erosion. In definition, opening is made up of erosion followed by dilation by using the same structuring element. The effect of the operator is to preserve foreground regions that have a similar shape to this structuring element, or that can completely contain the structuring element, while eliminating all other regions of foreground pixels [33].

The opening of an image  $I$  by structuring element,  $\hat{S}$ , denoted  $I \circ \hat{S}$ , is defined in the following equation

$$I \circ S = (I \otimes S) \oplus S$$

Closing is another important mathematical morphology operation. It is also derived from fundamental morphology operation dilation and erosion. In definition, it is made up of dilation followed by erosion with same structuring element. As the opposite of opening, the effect of the operator is to preserve background regions that have a similar shape to this structuring element, or that can completely contain the structuring element, while eliminating all other regions of background pixels.

The closing of an image  $I$  by structuring element,  $S$ , denoted  $I \cdot S$ , is defined in the following equation

$$I \cdot S = (I \oplus S) \otimes S$$

iii. *Top-hat and Bottom hat*

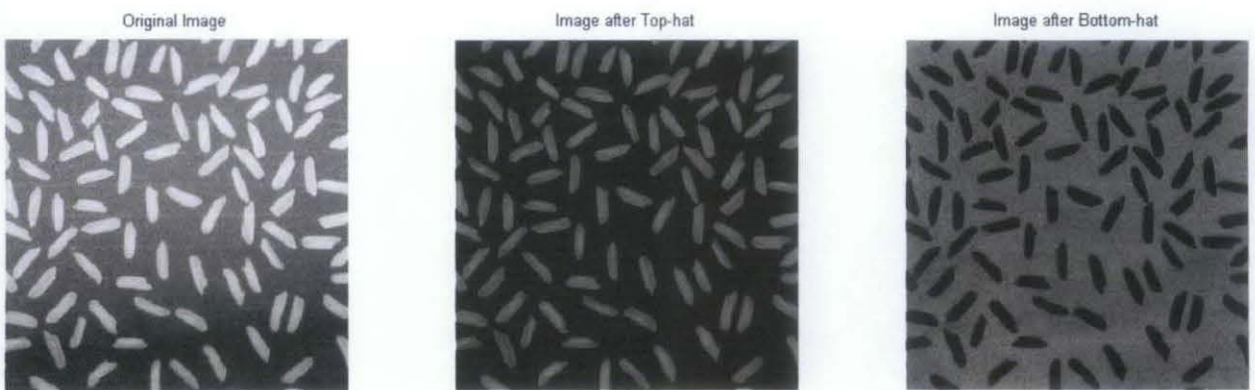
Top-hat and bottom hat transforms are popularly used for various image processing tasks, such as feature extraction, background equalization, image enhancement, and others. The top-hat transform is defined as the difference between the input image and its opening by some structuring element while bottom-hat transform is defined dually as the difference between the closing and the input image.

Top Hat :  $T(I, S) = I - (I \circ S)$

Bottom Hat :  $B(I, S) = (I \cdot S) - I$

$I(x,y)$  : *Input Image*

$S(x,y)$  : *Structuring Element*



(a) Original Image

(b) After Top-hat

(c) After Bottom-hat

Figure 24 Morphological Operation

## 2.4.2 Model based Approaches

Model based approach can basically be divided into two main category which are the parametric model and the geometric deformable model. The parametric model is preferable to segment image objects having uneven gray scale such as fundus images [34] while the geometric model using only geometric computations for the curve evolved instead of using any parameterization.

### 2.4.2.1 Parametric Model

The most common parametric model based approach is active contour model, or snake. It is defined as an energy minimizing spline [35]. The snakes energy depends on its shape and location within the image. Snakes may also be understood as a special case of a more general technique of matching a deformable model to an image by means of energy minimization [35]. Snakes is depending on other mechanism such as interaction with a user, interaction with some higher-level image understanding process, or information from image data adjacent in time or space and do not solve the entire problem of finding contours in images.

Interaction with user is important by providing an approximate shape and starting position for the snake somewhere near the desired contour. The priori will then push the snake towards an appropriate solution. These interactions make snakes becomes “active” compare to other image models It also exhibiting dynamic behaviour due to its characteristic which always minimized its energy functional.

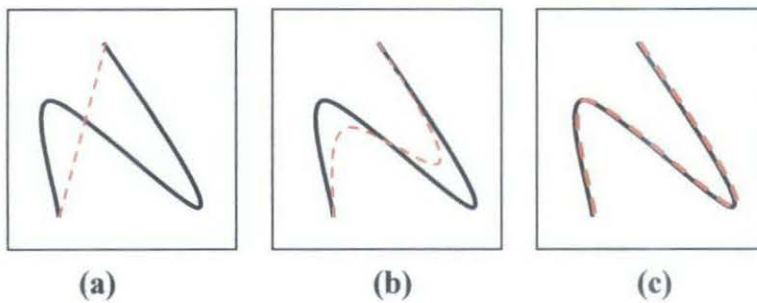


**Figure 25 Active Contour Model**

**(a) initial snake position (b) the snake is pulled towards the true contour (c) the snake matche the true contour**

There are several types of active contour model being used as an effective tool for segmentation which will be discussed in the following subsection.

*i. Traditional snakes and balloons*

The energy functional which is minimized is a weighted combination of internal and external forces [35]. Generally, the external forces come from the image or from higher level image understanding process while the internal forces originate from the shape of the snake. The energy function can be expressed by the following equations

$$\text{Snake} \rightarrow \mathbf{v}(s) = [x(s), y(s)]$$

where  $x(s), y(s)$  are  $x, y$  co-ordinates along the contour

$$\begin{aligned} \text{Energy} \rightarrow E_{snake}^* &= \int_0^1 E_{snake}(v(s)) ds \\ &= \int_0^1 (E_{int}(v(s)) + E_{image}(v(s)) + E_{con}(v(s))) ds \end{aligned}$$

Where  $E_{int}$  represents the internal energy of the spline due to bending,  $E_{image}$  denotes image forces, and  $E_{con}$  shows external constraint forces. A demonstration of Snake operation is shown below

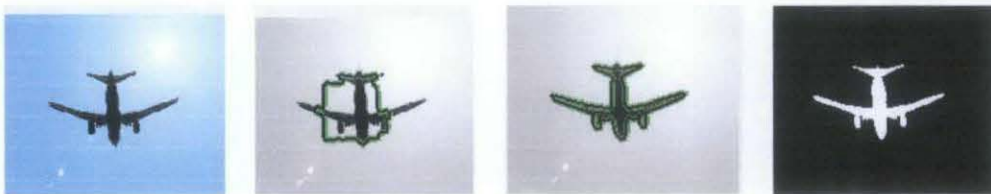


**Figure 26 Demo of Snake Opetations**

The traditional snake has some difficulties with the numerical instability. However, this problem has been solved by Berger [36] by incorporating an ideal of snake growing. A different approach to the energy integral minimization has proposed in [37]. It has greater numerical stability and better efficiency. An additional pressure force is added to the snake to overcome isolated energy valley resulting from spurious edge points, giving a better result. This additional forces is added by considering the curve as a balloon which is inflated [35].

There are plenty of researchers using Snakes as the method for medical image segmentation such as segmenting human left ventricle from echocardiography image [38]. However, most of these researchers have modified the traditional snakes in order to achieve higher accuracy and efficiency. For example, in [38], they have combining snakes and active snake models to obtain better results.

ii. *Gradient vector flow snakes*

Gradient vector flow snake have overcomes two main limitations of the traditional snakes which are the requirement of snake initialization being close to the desired solution, and difficulties in segmenting concave portions of the boundary [35].

GVF field is a non-irrotational external force field that points towards the boundaries when in their proximity and varies smoothly over homogeneous image regions all the way to image borders. As a result, it can actually drive a snake toward a border from a large distance and can segment object concavities. To achieve this, GVF snake does not need to carefully fine tune the balloons forces to overcome the noise but not overcome the salient image features, and can attract the snake when initialized at either side of the boundary. The GVF snake is insensitive to initialization and able to segment concave boundaries result [35]. It can be represented by the following energy equation:

$$\text{GVF Field} \rightarrow \mathbf{g}(x, y) = (u(x, y), v(x, y))$$

$$\text{Energy} \rightarrow E = \iint \mu (u_x^2 + y_y^2 + v_x^2 + v_y^2) + |\nabla f|^2 |g - \nabla f|^2 dx dy$$

Where  $\mu$  is a regularization parameter balancing the weight of the first and second term.

iii. *Water flow*

The water flow technique is based on the paradigm of water flow [39]. The force field analogy which similar to Snake is used to implement the major water flow attributes such as water pressure, surface tension, and adhesion so that the model achieves topological adaptability and geometrical flexibility. This snake like force functional combining edge and region based forces is introduced to produce capability for both range

and accuracy [39]. It has the ability to handle noise and being tested on many types of medical images such as femur, brain, carotid artery, and fundus images (See the figure below).

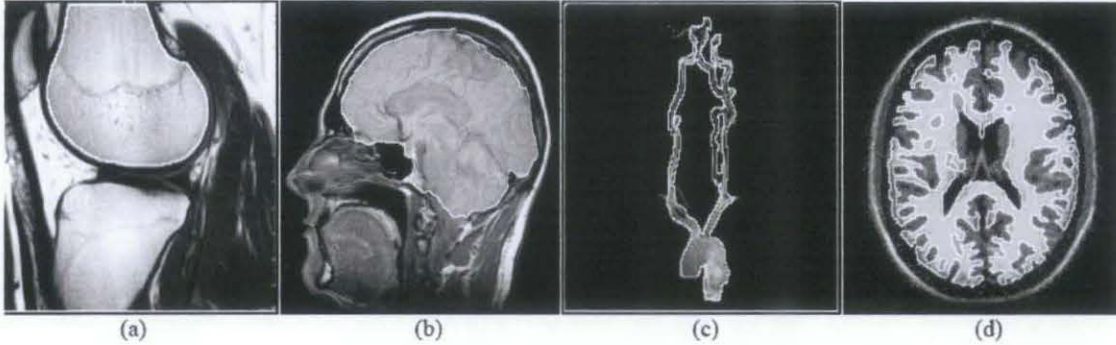


**Figure 27 Segmentation results for water flow method**

(a)Femur in MR knee image, (b)brain in a sagittal MR Image, (c) carotid artery in a MR carotid MRA image, and (d) grey/white matter interface in MR brain image slice  
(image adapted from [40])

In this approach, one pixel in the image is considered to be one basic unit of the water. The water pressure is defined as the resultant force of the repulsive force between the water elements. The elements on the water contour, however, are considered to attract other contour elements, and hence generate surface tension [40].

The flow process is made up by two steps which are first, acceleration (the contour element achieves a velocity due to the presence of the water pressure, surface tension and adhesive force ) and second, exterior movement where the moving element is now free from the influence of other water elements and suffers only external image forces [40].

#### 2.4.2.2 Geometric Deformable Models

The main criteria that separate geometric deformable model from parametric deformable model is that curves are evolved using only geometric computations instead of any parameterization [35].Consequently, the curves can be represented as level sets or higher dimensional functions yielding seamless treatment of topological changes.

This approach presents several advantages over the traditional parametric active contours.

First, the contours represented by the level set function may break or merge naturally during the evolution, and the topological changes are thus automatically handled. Second, the level set function always remains a function on a fixed grid, which allows efficient numerical schemes [41].

There are several types of geometric deformable models such as level set method and geodesic method. The most fundamental method for geometric deformable models is level set method which will be discussed in the following subsection.

*i. Level Set Front Propagation*

Level set method is first introduced by Osher and Sethian [42] for capturing moving fronts. In level set formulation of moving fronts (or active contours), the fronts, denoted by  $C$ , are represented by the zero level set  $C(t) = \{(x, y) \mid \varphi(t, x, y) = 0\}$  of a level set function  $\varphi(t, x, y)$ . The evolution equation of the level set function  $\varphi$  can be written in the following general form:

$$\frac{\partial \varphi}{\partial t} + F|\nabla \varphi| = 0$$

which is called *level set equation* [42]. The function  $F$  is called the speed function. For image segmentation, the function  $F$  depends on the image data and the level set function  $\varphi$ .

In traditional level set methods, the level set function  $\varphi$  can develop shocks, very sharp and/or flat shape during the evolution, which makes further computation highly inaccurate [41]. To avoid these problems, a common numerical scheme is to initialize the function  $\varphi$  as a signed distance function before the evolution, and then “reshape” (or “re-initialize”) the function  $\varphi$  to be a signed distance function periodically during the evolution. Indeed, the reinitialization is crucial and can not be avoided when using traditional level set method. Hence, there are several papers has came out several modifications such as in [41], they forces the level set function to be close to a signed distance function, and therefore

completely eliminates the need of the costly re-initialization procedure.

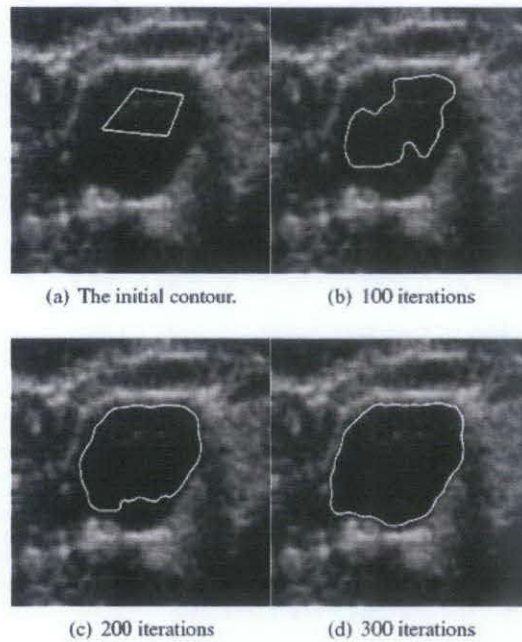


**Figure 28 Result for an ultrasound image of carotid artery using Level Set Method**

(image adapted from [41])

### 2.4.3 Tracking based approaches

Tracking based approaches are very similar to pattern recognition approach except they apply locally instead of global operator. This method utilizes a profile model to incrementally step along and segment a vessel. In [43], a Hough transform is used to locate the papilla in retinal image. Vessel tracing proceeds iteratively from the papilla, halting when the response to a one-dimensional (cross-section) matched filter falls below a given threshold. In [44], the tracking based method was employed to extract vessel in coronary arteriogram, from user defined starting points.

The disadvantage of this method is their proclivity for termination at branch points (whether real or caused by pathology), which are not detected well by 1-D filters [29]. On the other hand, their reliance upon unsophisticated methods for locating the starting points, which must always be either at the optic nerve or at subsequently detected branch points will be another draw for this method [29].

#### *2.4.4 Neural network based approaches*

Neural network method is based in the use of sample patterns to estimate statistical parameters of each pattern class. The minimum distance classifier is specified completely by the mean vector of each class. The patterns used to estimate these parameters usually are called training patterns, and a set of such patterns from each class is called a training set. The process where decision functions is obtained by using the training set is called learning or training [22].

This method is an efficient segmentation method for diagnosis such as breast cancer [45], diabetic retinopathy [46], and etc. The main disadvantage of this method is it requires a good image database for each diagnosis for its accuracy. The unavailability of image database will definitely reduce the accuracy of this technique.

#### *2.4.5 Other approaches*

Besides the common categories that have been discussed at the previous sub section, there are also some image segmentation methods that has been done by some researcher such as fuzzy logic [47] which is very useful to the medical industry for diagnosis and medication.

## 2.5 Analysis Method for Retinal Image

Retinal Image is one of the favourite areas for the researchers to analyse for diagnostic purposes. From the studies, there are several features of retinal images used to detect diseases such as diabetes and hypertension. The following are the features that being used for diagnosis purposes:-

### 2.5.1 Exudates

Exudates are white spots appeared in the retinal images (Please refer to Figure 29). From the research, the feature of exudates is associated with both hypertension and diabetes [48].

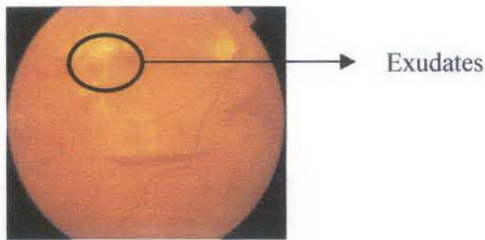


**Figure 29 Retinal Exudates**

(Image Adapted from [49])

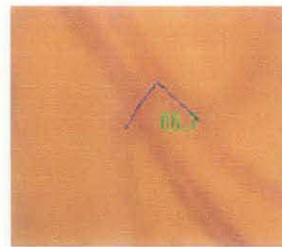


**Figure 30 Bifurcation angle**

(Image adapted from [49])

### 2.5.2 Bifurcation angle

Bifurcation angle reflect the change of an optimal branching arrangement caused by diseases [49]. From the studies, detection of numbers of obtuse angle will help doctor in the clinic diagnosis [49].

### 2.5.3 Mean arteriolar and vein diameters and artery-to-vein diameter ratio

The arterial and vein diameters refer to the dimension of the parts between the optic disc and the first bifurcation of the vessels [49] (Please refer to figure 32). This feature will pathologically changed for hypertensive patients and useful for diagnosis [49].

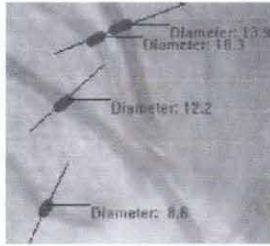


**Figure 32 arterial and venal diameter measurement**

(Image adapted from [48])

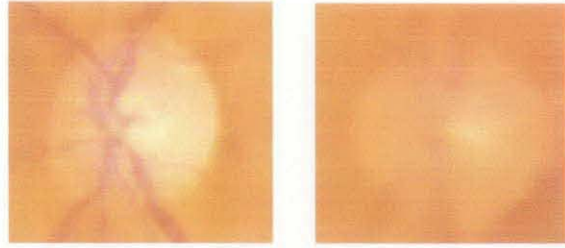


**Figure 31 Size of optic disc for hypertensive and diabetic**

(Image adapted form [49])

#### 2.5.4 Shape and size of optic disc and cup

The shape and size change of the optic disc and the optic disc to cup ratio (Refer to figure 31) may be features to detect hypertension or diabetes.

#### 2.5.5 Vessel Tortuosity

The retinal blood vessels normally largely straight or gently curved. In some diseases, it will become tortuous [48] (example shown in figure 33). Tortuous refer to the blood vessel become dilated and take on a wavy path [49].

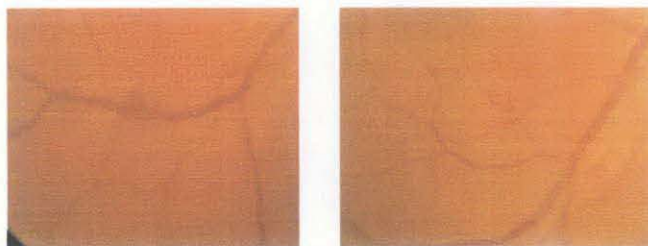


**Figure 33 Tortuous for hypertensive and diabetic**

(Image Adapted from [49])

## CHAPTER 3

### METHODOLOGY

#### 3.1 Project Methodology

From the studies and research, the process of this project has been identified and shown below. The overall project has been divided into 4 main parts. It generally consists of the design and development of the algorithm for segmentation and feature extraction of the retinal vasculature. All these parts will be performed throughout semester 1 and semester 2.

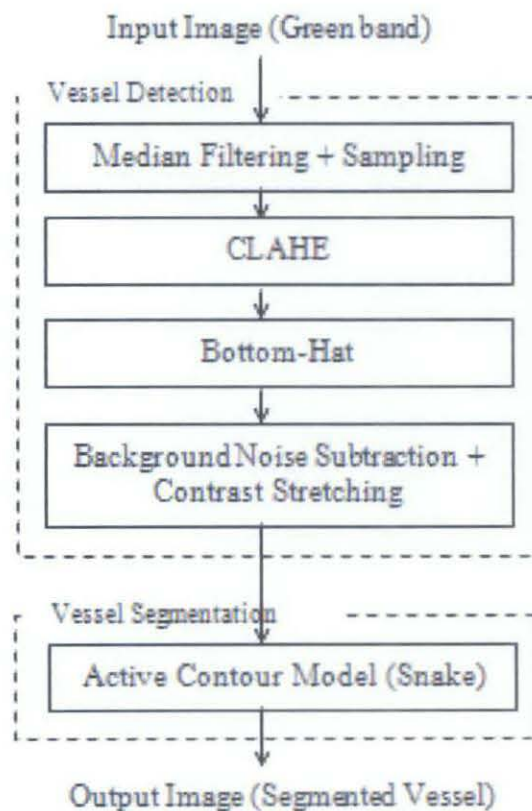
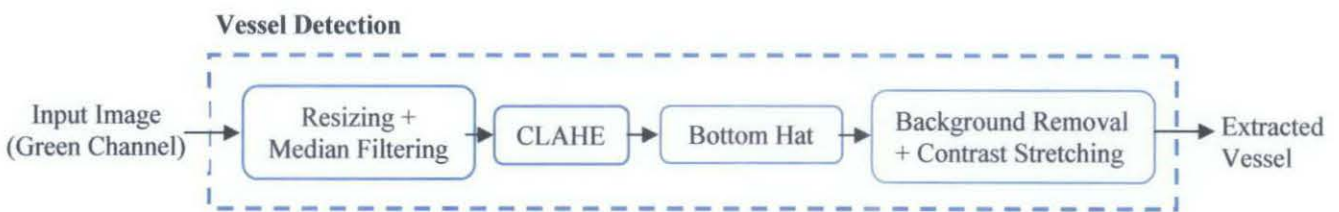


Figure 34 Design Process

### 3.2 Vessel Detection Phase

The structure of retinal vessel plays an important role in diagnosing hypertension and other eye diseases such as diabetes. In this chapter, the methods for developments of extraction of retinal vessel using image processing techniques are being presented (as shown in the Figure 35). Vessel extraction in this case refers to the process of separating the retinal vasculature from the background. The result will be an image which the extracted vessels are of higher intensity level and well contrasted from its background.



**Figure 35 Vessel Detection Phase**

#### 3.2.1 Reference Model Images

In this stage, a reference retinal image is being used, namely Reference TIF Fundus Image. This image is used to test on the algorithm (See figure 30).

As shown in the Figure 36, the Reference TIF Fundus Image is a 24-bit TIFF format typical colour image of retinal. This consists of 8-bits red, green, and blue layers with 256 levels each. This reference image is obtained from the DRIVE database [50].



**Figure 36 Reference Fundus Image (TIF Format)**

### 3.2.2 Pre-processing (Image Enhancement)

Pre-processing and image enhancement processes are very important prior to the actual vessel extraction. A RGB colour fundus image has 3 intensity plane which are red, green and blue channels. A colour plane needs to be selected in order to proceed to the other image enhancement and segmentation processes.

Prior to enhancement, a combination of geometric operation and median filtering is performed. The main reason of using median filter is to reduce spurious noise and to smooth out the transition intensity mostly at vessel borders while preserving vessel edges. The images has been enlarged by two using bi-cubic method, filter by median filter then resized back to its original size. The enlargement process is to avoid missing of detail vessel after the median filtering process.

For image enhancement, contrast stretching is needed at early stage to obtain a desired range for intensity gray level. Due to the non-uniform background of the fundus images, Contrast Limited Adaptive Histogram Equalization (CLAHE) is selected (as described in Chapter2) to evenly enhanced the bright region and the dark region.

### 3.2.3 Vessel Detection

The task to detect vessel from the background become less difficult after the contrast enhancement. The enhanced vessels in green channel are appears as dark colour object. To extract these vessel, the morphological operation, Bottom-hat is used. The operation can be expressed as follows:

$$\begin{aligned} \text{Closing} & \quad I \cdot S = (I \oplus S) \otimes S \\ \text{Bottom Hat} & \quad : \quad B(I, S) = (I \cdot S) - I \end{aligned}$$

In bottom-hat operations, we perform closing of the image,  $\tilde{I}(x,y)$  by a structuring element,  $S(x,y)$  followed by subtraction by input image  $I(x,y)$ . Note that the closing

operation is defined as the dilation operation followed by erosion operation by using the same structuring element as described in Chapter2.

In this operation, the structuring element used is line type. The size of the element is set to be 15 based on the typical size of the branching points and intersection points. The primary vessels are normally 10-12 pixels wide but branching and intersection points will have 2-3 pixels extra in width.

Orientation is the other important parameter for structuring elements. Bottom hat operation is performed at several orientations to ensure vessels at different orientation are extracted. If the orientation is assigned every 15 degrees, this will make the total number of Bottom hat operations to be 12. The resultant images will be summed to obtain a sum of Bottom-hat. There are several example of structuring elements with size 5 shown below:

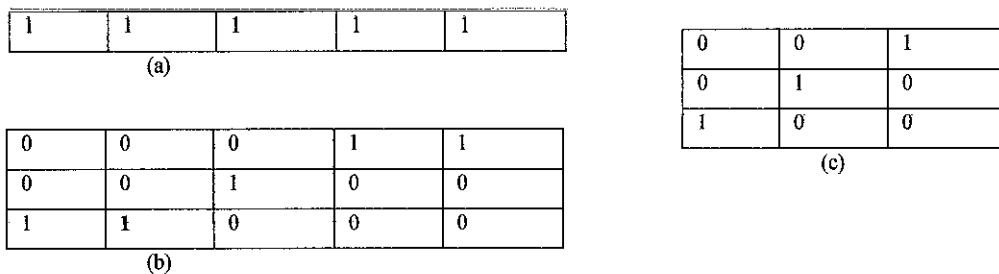


**Figure 37 Linear structuring element**

**(a) Size=5, Orientation = 15 degrees, (b) Size = 5, Orientation = 45degrees, (c) Size = 5, Orientation = 45 degrees**

The extracted vessels are estimated as follows:

$$\text{Sum of Bottom-hat } (I, B_{12}) = \sum_{i=1}^{12} ((I \cdot B_i) - I)$$

After CLAHE, a process called background removal has performed to reduce the artifacts caused by the contrast enhancement process. This process performs by subtracting the sum of Bottom hat image by its background image. The background image is obtaining by using averaging filter of size 50x50 pixels to the sum of bottom hat image. This filter is able to suppress the foreground information that is mainly the blood vessels. Then, contrast

stretching is then performed to increase the contrast between the blood vessels and its background. The vessel now is considered extracted.

### 3.3 Vessel Segmentation Phase

From the result of vessel detection phase, it has portrayed several weaknesses such as the artifacts in the surroundings are being highlighted while the bifurcation and intersection points are unable to be highlighted effectively. The main reasons are the production of artifacts due to CLAHE and the profiles are larger than the structural element for morphological operation respectively.

Vessel segmentation phase has been implemented in order to solve the above matter. The proposed method for the vessel reconstruction phase is an active contour model (Snake) that based on level sets, techniques of curve evolution, and Mumford-Shah functional for segmentation. This approach is one of the segmentation methods that can extract targeted objects from a noisy environment [51]. On the other hand, this method do not required smoothing of initial image which makes the location of boundaries are well preserved and detected.

The general description of the proposed vessel reconstruction method is based on the following equation. We assumed that a 2D retinal image consisting of pixels  $I(x,y)$  and the segmentation defined by an evolving closed zero level set curve  $\emptyset$ , the energy functional [51] is

$$\begin{aligned} C(\emptyset, a_1, a_2) &= C_1(\emptyset, a_1, a_2) + C_2(\emptyset, a_1, a_2) \\ &= \int_{\text{inside}(\emptyset)} (I(x,y) - a_1)^2 dx dy + \int_{\text{outside}(\emptyset)} (I(x,y) - a_2)^2 dx dy \end{aligned}$$

From the above equation, the constants  $a_1, a_2$  represent the mean intensities of the interior and exterior of the segmented object(s). When the zero-level set  $\emptyset$  coincides with the object boundary and best separates the object and background with respect to their mean intensities, the energy  $C(\emptyset, a_1, a_2)$  is minimized.

There are several conditions for the location of the curve which have been illustrated in Figure 3. If the curve  $\emptyset$  is inside the object, then  $C_1(\emptyset) \cong 0$  and  $C_2(\emptyset) > 0$ . If

the curve  $\emptyset$  is outside the object, then  $C_1(\emptyset) > 0$  and  $C_2(\emptyset) \cong 0$ . If the curve  $\emptyset$  is both inside and outside of the object, then  $C_1(\emptyset) > 0$  and  $C_2(\emptyset) > 0$ .

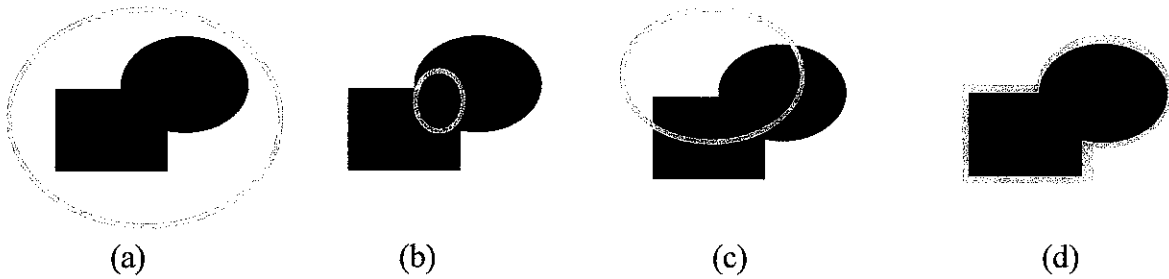


**Figure 38 Conditions for the Energy Function**

- (a)  $C_1(\emptyset) > 0, C_2(\emptyset) \cong 0$     (b)  $C_1(\emptyset) \cong 0, C_2(\emptyset) > 0$     (c)  $C_1(\emptyset) > 0, C_2(\emptyset) > 0$   
 (d)  $C_1(\emptyset) \cong 0, C_2(\emptyset) \cong 0$

The main objective of the vessel segmentation phase is also to segment only retinal vessels with accurate identification at the vessel borders in binary. For this method, it can be either interactive with user or fully automated by selecting either presetting the initial contour and starting point or letting the user to define it himself. In our proposed method, the initial contour is set priory in order to make this algorithm fully automated. The shape and position of the initial contour will directly affect the result of the vessel segmentation phase [51]. As a result, an initial contour has been designed to fit the complex structure of retinal vasculature which shown in Figure 4.

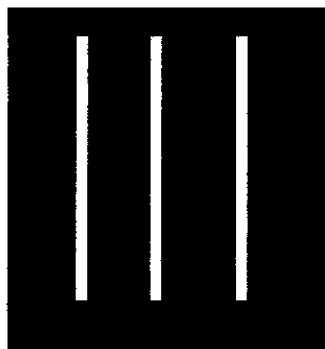


**Figure 39 Initial Contour**

The main reason behind this design of initial contour is to cover most of the area in the retinal vasculature. It will leads to a higher accuracy result compare to initial contour that only focus at centre or one side.

Besides the initial contour, there is another condition that will affect the quality of the result which is the number of iterations for the calculation of the energy function. The number of iterations will have an impact on the quality of the image as well as the computational time. For our design, the number of iterations has been set to 1000 due to the complexity of the retinal vasculature.

### 3.4 Performance Analysis of Detection and Segmentation of Retinal Vasculature

The developed algorithm is analyzed using the DRIVE database [50] and benchmarked against manual approach as well as other published algorithms. For performance analysis, the reconstructed vessels by the algorithm and the manually segmented image by the first observer are considered.

Let  $C(x,y)$  be the automatically reconstructed image by the algorithm, and the  $G(x,y)$  be the manually segmented image of set A from DRIVE database. A vessel pixel when reconstructed as a vessel is considered as TP. However, a non-vessel pixel when reconstructed is considered as FP. Meanwhile, TN is when a non-vessel is reconstructed as non-vessel which FN is when a vessel pixel is reconstructed as non-vessel. All the parameters are determined below:

$$TN: \sum_{all\ x,y} [C(x,y) = G(x,y) = 0]$$

$$TP: \sum_{all\ x,y} [C(x,y) = G(x,y) = 1]$$

$$FN: \sum_{all\ x,y} [(C(x,y) = 0) \cap (G(x,y) = 1)]$$

$$FP: \sum_{all\ x,y} [(C(x,y) = 1) \cap (G(x,y) = 0)]$$

The performance parameters are as follow [50]:

$$TN\ Fraction : \frac{\sum_{all\ x,y} [C(x,y) = G(x,y) = 0]}{\sum_{all\ x,y} [C(x,y) = 0]}$$

$$TP\ Fraction : \frac{\sum_{all\ x,y} [C(x,y) = G(x,y) = 1]}{\sum_{all\ x,y} [C(x,y) = 1]}$$

$$\text{FN Fraction : } \frac{\sum_{all\ x,y}[(C(x,y)=0) \cap (G(x,y)=1)]}{\sum_{all\ x,y}[(C(x,y)=0)]}$$

$$\text{FP Fraction : } \frac{\sum_{all\ x,y}[(C(x,y)=1) \cap (G(x,y)=0)]}{\sum_{all\ x,y}[(C(x,y)=1)]}$$

The above values is being used to calculated the other three parameters which are accuracy, specificity, and sensitivity.

$$\text{Accuracy} = (\text{TP} + \text{TN}) / \text{FOV}$$

$$\text{Specificity} = \text{TN} / (\text{TN} + \text{FP})$$

$$\text{Sensitivity} = \text{TP} / (\text{TP} + \text{FN})$$

Where FOV (field of view) is the circular with diameter of approximately 540 pixels. Under segmentation leads to a higher FN while over segmentation leads to a higher FP fraction. Ideally, the performance of a segmented algorithm that segments foreground and background should results in small FP and FN fraction (FP, FN  $\rightarrow$  0) and large TP and TN fractions (TP, TN  $\rightarrow$  1).

### 3.5 Tools

This project is focusing on diagnosis and analysis using image processing technique. For carrying out this project, several tools identified as the requirement. The following are the tools needed:

**Table 3 Tool Needed for the Project**

Tools		Description
Software	MATLAB	A programming language for technical computing from The MathWorks. Its Image Processing tool box is very useful for image analysis and its GUI Toolbox can be used to create a user friendly interface.
Hardware	KOWA Fundus Camera Non-Myd7 (Refer to Appendix A2)	A specialized low power microscope with an attached camera designed to photograph the interior surface of the eye, including the retina, optic disc, macula, and posterior pole.

### 3.6 Key Milestones

The key milestone for the project is summarized in the Gantt chart (Please refer to APPENDIX A).

## CHAPTER 4

### RESULTS AND DISCUSSION

#### 4.1 Results

##### 4.1.1 Vessel Detection Phase

##### 4.1.1.1 Pre-processing (Image Enhancement)

When the reference images are separated into their channels (Red, Green, and Blue), the green channel provided the best contrast of vessel to its surrounding as shown in figure 32. Besides, the green channel also provided better contrast compared to the overall gray level image. As a result, the green channel of the image was extracted as the first step in pre-processing stage.

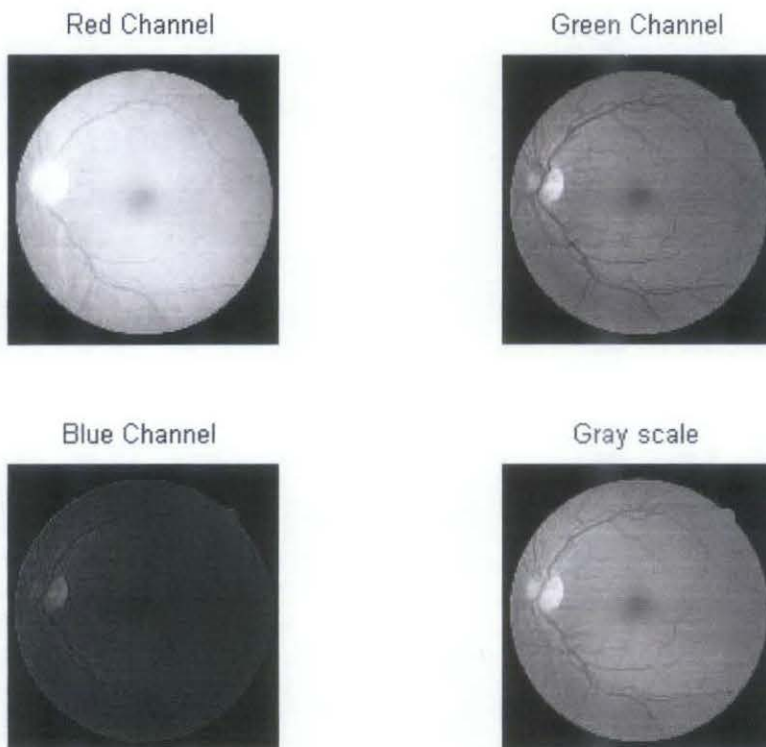
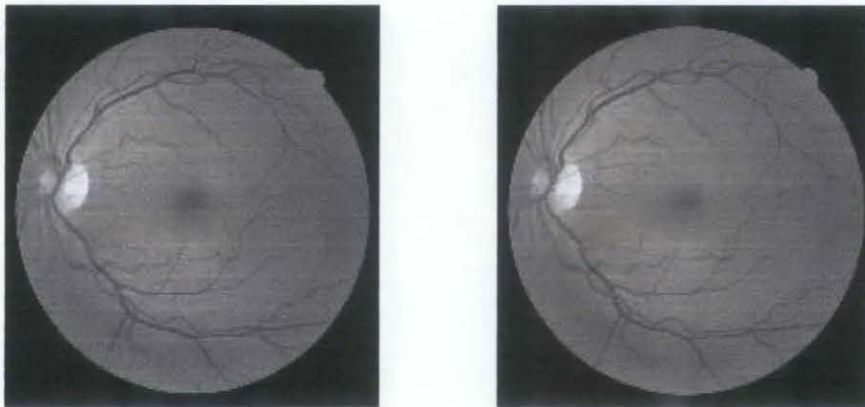


**Figure 40 Colour channel for TIF format**

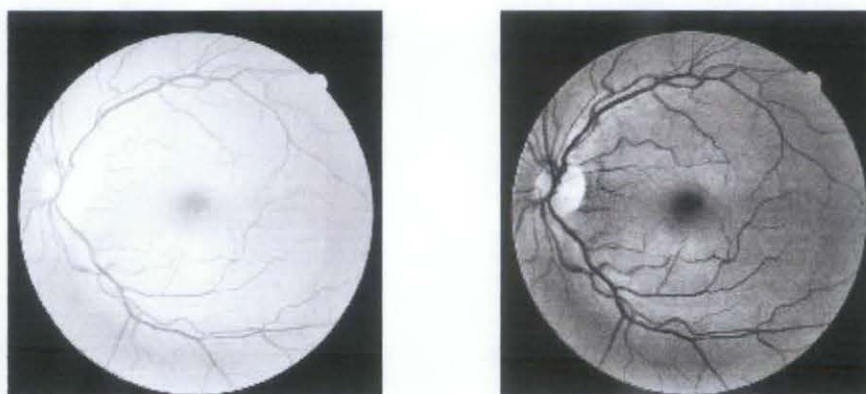
After enlarged the image by two using bi-cubic method, then filtered the image by median filter, and resized back to its original size, (as shown in figure 33), the image was smoothed while preserving the edges. The application of the mean filter in this step was mainly to ensure reconstructed vessel borders are well defined.



**(a) Green Channel**                      **(b) After median filtering**

**Figure 41 TIF Image for Median Filtering**

Then, contrast enhancement process was performed. From the results, it shows that contrast stretching was not reliable for contrast enhancement for fundus images as fundus image was high in variability and poor in proper illumination while the window based enhancement technique, CLAHE was contrasting effectively on each part of the fundus image. That was because it applied histogram equalization within small windows in the image and ensured hidden features within the windows be more visible.



**(a) After Contrast Stretching**                      **(b) After CLAHE**

**Figure 42 TIF Image for contrast enhancement**

#### 4.1.1.2 Vessel Detection

After image enhancement process, the image segmentation process was performed to detect vessel from the background. From the result shown in the Figure 35, it can be observed that there was still non-vessel structures such as added background linear features and some artifacts in the background were being highlighted as well. The artifacts were produced after CLAHE. In addition to this, there were also some intersection and branching points which are weakly extracted.

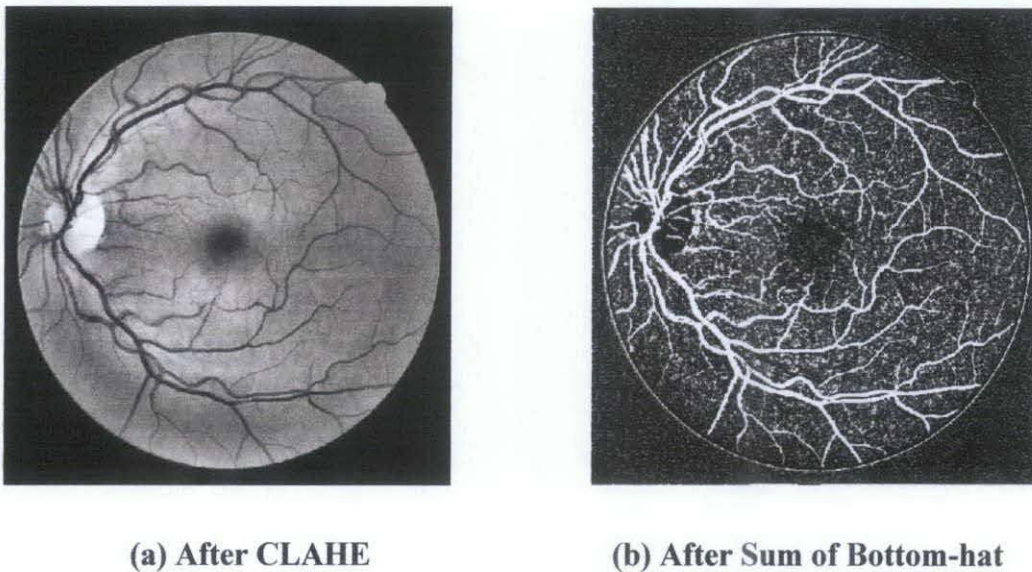
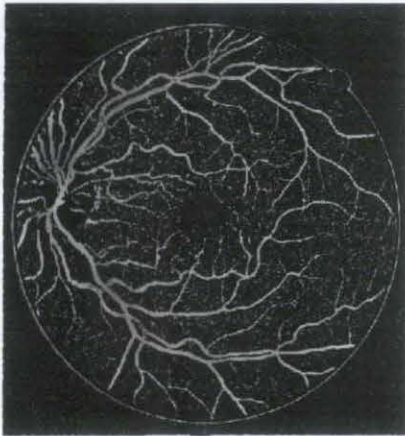
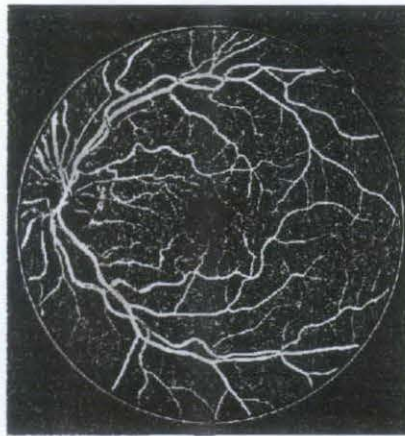


**Figure 43 TIF Image after morphological operation**

In order to reduce the artifacts, a process called background removal was performed. From the results, the artifacts were reduced. Then, contrast stretching was performed to increase the contrast between the blood vessels and its background. After the discussed processes, the vessel was considered extracted.



**(a) After Background Noise Removal**



**(b) After Contrast Stretching on the Background Noise Removed Image**

**Figure 44 TIF Image after background removal process**

#### **4.1.2 Vessel Segmentation Phase**

Due to the limitation from the morphological operations, active contour model is used to obtain the vessel from the noisy background. The process was performed on the image after sum of bottom hat morphological operations. The initial contour is preset and the number of iterations is set to 1000. 1000 iterations is an ideal number of iterations because when the number more than 1000, the result might be over segmented and the computational time will increase and affect the efficiency of the diagnosis algorithm. On the other hand, if the number of iterations less than 1000, the accuracy of the segmented vessel will reduce although the computational time has reduced. The resultant image consists of the desired contour and the background.

The result of the active contour model segmentation is shown in the following figure. In analyzing the results from the Active Contour Model, Snake, it is found out that problems like over-segmentation and false detection still occurred. The false detection is due to the poor pre-processing method that creates artifacts. Besides, over segmentation is occurred due to the size of the structuring element used in morphological operations.

Because the branching and intersection points are larger than the primary vessels, the size of the structuring element is set larger than the primary vessels and this resulted in the extraction of vessel borders that has been expanded due to CLAHE [23].

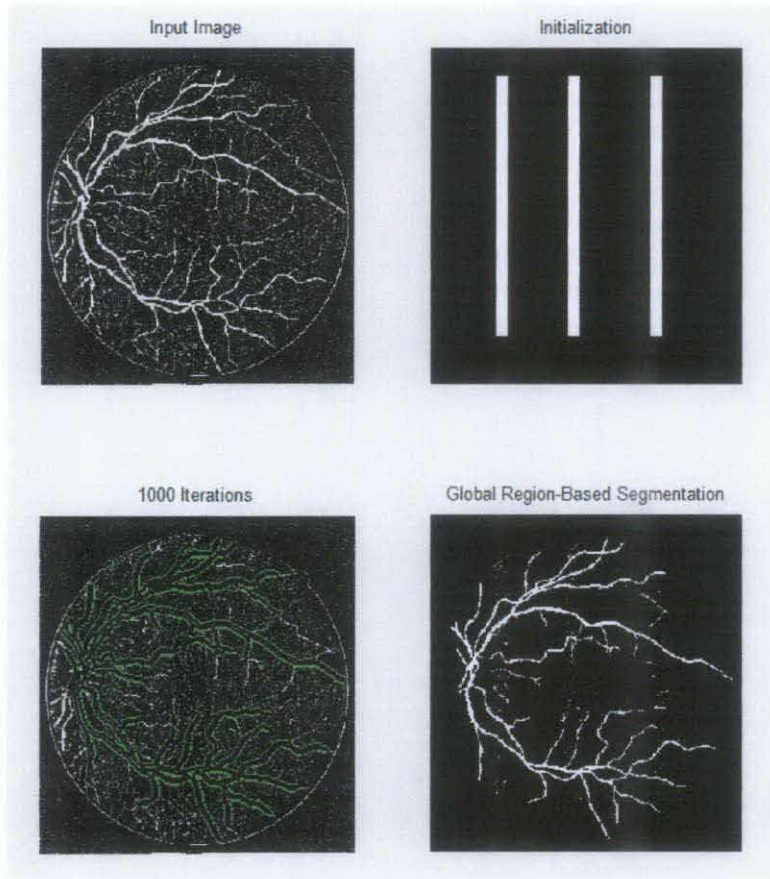


**Figure 45 Results of Active Contour Model**

#### *4.1.3 Performance Analysis of Detection and Segmentation of Retinal Vasculature*

The algorithm has been tested on 20 images from DRIVE database, the TP, FP, TN, FN fractions, the accuracy, the sensitivity, and the specificity performance parameters are tabulated in the following table

From the result, it can be seen that the algorithm can detect and reconstruct vessel (sensitivity) at a mean of 93.08% and non-vessel (specificity) at a mean of 81.38%. Over segmentation (FP) is at a mean of 21.69% while under-segmentation (FN) is as low as 5.85%.

**Table 4 Performance parameters (based on 20 test images from DRIVE database)**

Image	MAA	TP	FP	TN	FN	SP	SE
1	0.9210	0.7396	0.2604	0.9431	0.0569	0.7836	0.9285
2	0.9262	0.7979	0.2021	0.9450	0.0550	0.8238	0.9355
3	0.9135	0.8289	0.1711	0.9219	0.0781	0.8435	0.9139
4	0.9342	0.8205	0.1795	0.9476	0.0524	0.8407	0.9400
5	0.9272	0.8451	0.1549	0.9354	0.0646	0.8580	0.9290
6	0.9176	0.8364	0.1636	0.9254	0.0746	0.8497	0.9181
7	0.9197	0.7904	0.2096	0.9325	0.0675	0.8165	0.9213
8	0.9194	0.8242	0.1758	0.9265	0.0735	0.8405	0.9182
9	0.9319	0.8288	0.1712	0.9402	0.0598	0.8460	0.9327
10	0.9295	0.7840	0.2160	0.9432	0.0568	0.8137	0.9325
11	0.9196	0.7287	0.2713	0.9426	0.0574	0.7765	0.9270
12	0.9271	0.7898	0.2102	0.9407	0.0593	0.8174	0.9301
13	0.9205	0.8001	0.1999	0.9344	0.0656	0.8238	0.9242
14	0.9316	0.7368	0.2632	0.9544	0.0456	0.7838	0.9418
15	0.9364	0.7129	0.2871	0.9597	0.0403	0.7697	0.9465
16	0.9278	0.7871	0.2129	0.9438	0.0562	0.8159	0.9334
17	0.9268	0.7805	0.2195	0.9411	0.0589	0.8108	0.9299
18	0.9289	0.7196	0.2804	0.9521	0.0479	0.7725	0.9376
19	0.9313	0.7684	0.2316	0.9486	0.0514	0.8038	0.9373
20	0.9336	0.7423	0.2577	0.9509	0.0491	0.7868	0.9379
<b>Mean</b>	<b>0.9262</b>	<b>0.7831</b>	<b>0.2169</b>	<b>0.9415</b>	<b>0.0585</b>	<b>0.8138</b>	<b>0.9308</b>

Besides, the comparison of the developed algorithm with the other published methods based on the accuracy performance parameter is shown in the Table 5. This accuracy parameter is used to compare the performance of several methods in segmenting vessels in the database images with respect to the manually segmented image by the first observer.

If based on the accuracy parameter, this method is found comparable to other methods such as pixel classification [50] and by Zana [52]. From the observation, the pixel

classification [50] slightly outperforms other published methods including the developed algorithm. The main reason is because pixel classification [50] is a supervised method which needs to be trained by examples. However, there are limitations in developing rules that will work for all situations.

**Table 5 Accuracy achieved by the published methods reproduced from [50]**

Method	Mean Accuracy
2 <sup>nd</sup> observer [50]	0.9474
Pixel Classification [50]	0.9416
Zana [52]	0.9377
Developed Algorithm	0.9262
Jiang [53]	0.9212
Martinez-Perez et al. [54]	0.9181
Chaudhuri et al. [30]	0.8773

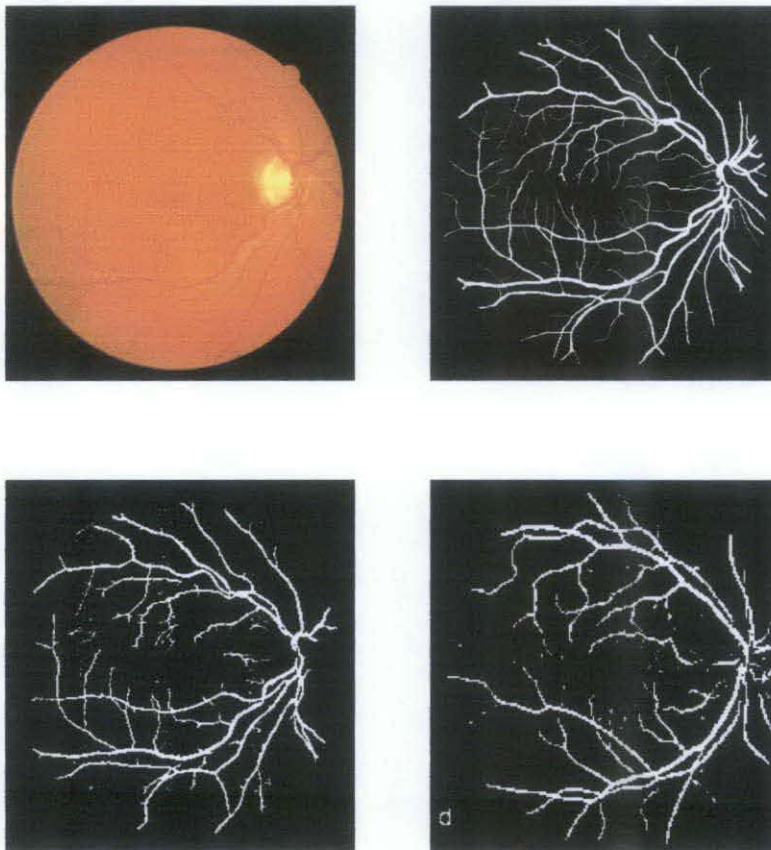
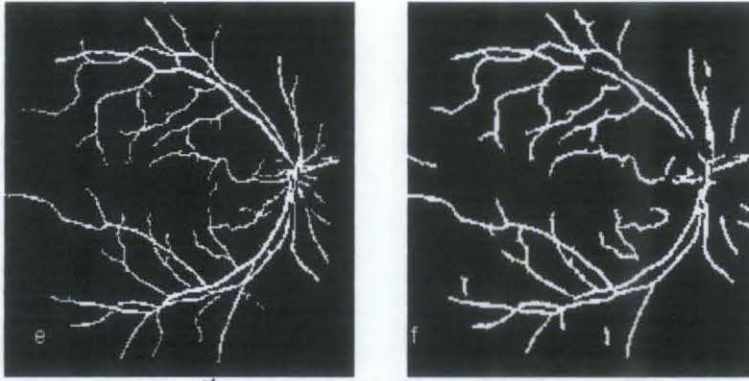


**Figure 46 Segmentation of one image from DRIVE database**



(a) Original image (b) 1<sup>st</sup> observer (c) developed algorithm (d) pixel classification

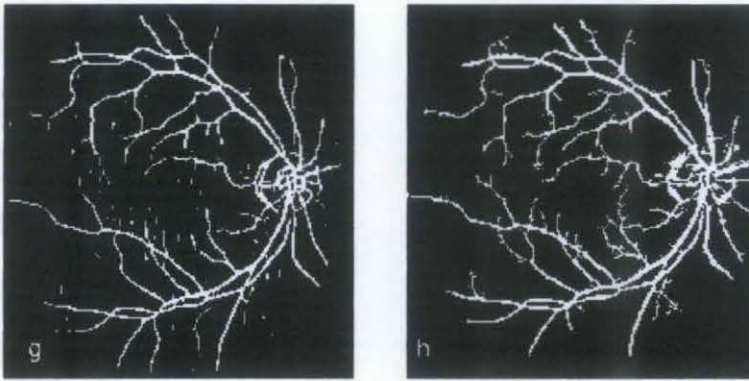


Figure 47 Segmentation of one image from DRIVE database

(e) Zana et al. (f) Jiang et al. (g) Chaudhuri et al. (h) Martinez-Perez et. al

The figures above depict the resultant image of segmentation and reconstruction of retinal vasculature by the developed algorithm, the 1<sup>st</sup> observer, and the published methods. The original image used in this figure is one of the images from the test set in DRIVE database.

Compare to 1<sup>st</sup> observer, over segmentation due to the optic disc can be seen in the result of Chaudhuri et al. and Martinez-Perez et al. while under segmentation of vessels in optic disc can be seen in the results of pixel classification [50] and Jiang [53]. False detection of vessels due to border of the camera's aperture can also be seen in the developed algorithm and Zana et al. [52].

#### 4.1.4 Graphic User Interface

In order to aid the user of this algorithm to perform the segmentation and visualize all the results from each phase, a graphic user interface has been created. The layout of the GUI is shown in Figure 6.

The control part in this GUI has been divided into two which are the image processing part and the performance analysis part. For image processing part, there are three buttons which loads image, detects vessel and segment vessel respectively according to our methodology of the algorithm. The results are then displayed in the first seven axes in the GUI.

For the performance analysis part, it is aimed to compare the segmented vessel with the benchmark from the online database. In this case, the performance analysis of the developed algorithm in segmenting retinal vessels of color fundus images from DRIVE database [50] is performed against the manually segmented retinal vessels from the 1<sup>st</sup> Observer of DRIVE database [50]. The results for the performance parameter are then displayed in the GUI as shown in Figure 6.

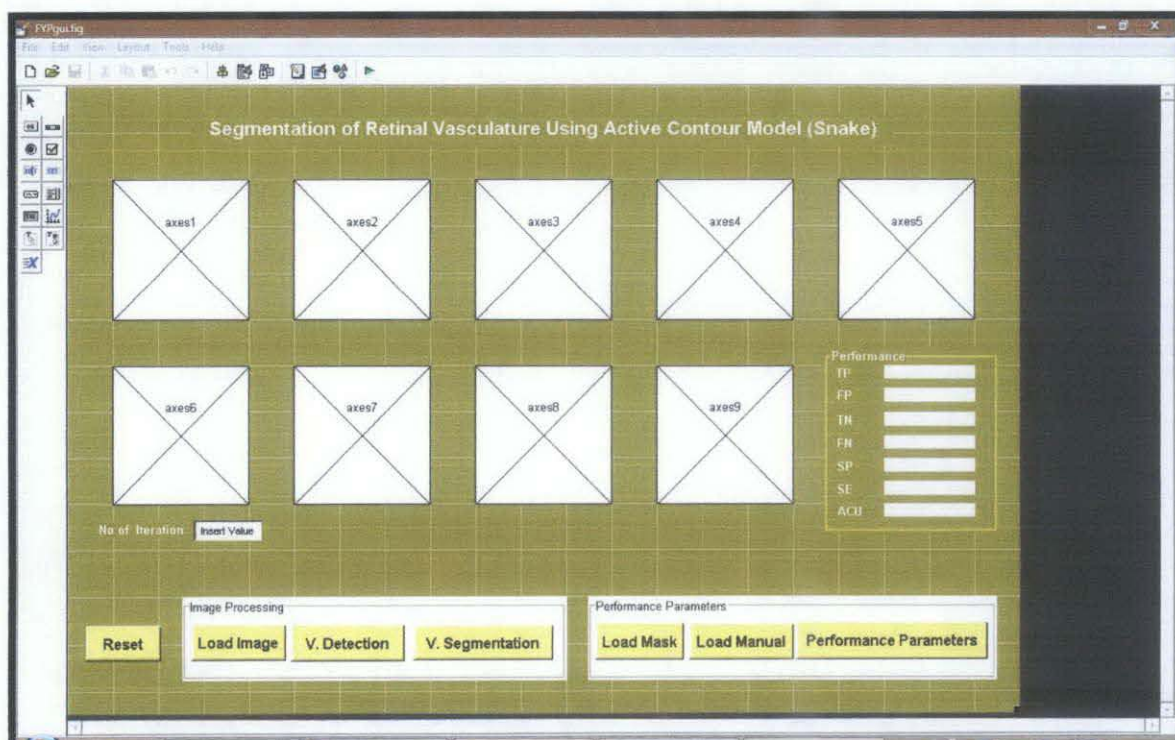


Figure 48 Development of Graphic User Interface

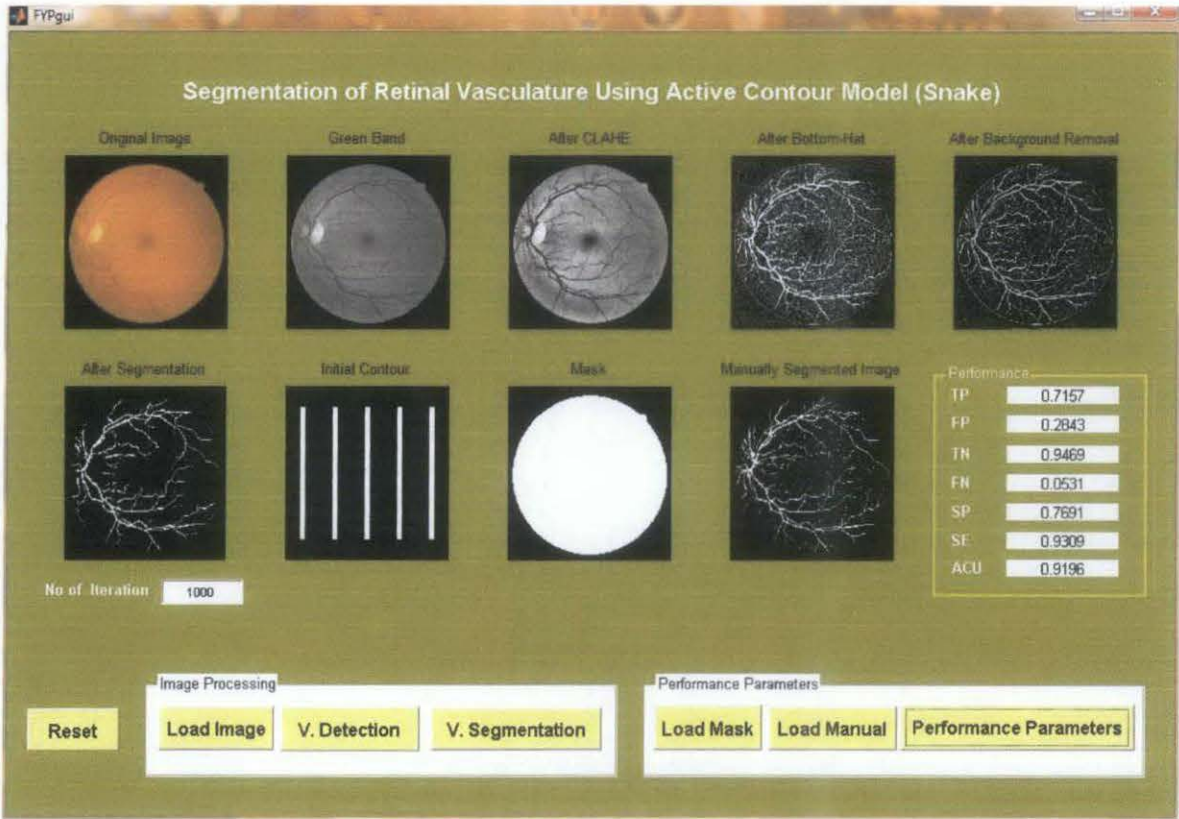


Figure 49 Layout of the GUI

## 4.2 Discussion

Prior to the detection and analysis of the retinal vessel morphology in fundus image, several steps have performed to enhance the vessel. First, to obtain smoother transition of intensity at vessel borders, median filtering has been applied to smoothen the image while remaining the important high frequency elements. To prevent one-pixel width vessels from being removed during median filtering, the size of the fundus image has increased to two times its original size. The median filtered image is resized back to its original size.

After that, CLAHE is used to enhance the contrast of vessels to its background in every region due to its window based nature. It produced a better results compare to histogram equalization and contrast stretching which are global based.

After vessel enhancement, sum of Bottom-hat is used to extract the vessel. A line type structuring elements with size 15 (the size of the maximum calibre of the branching point) with rotating angle  $0-180$  is used to ensure all vessels from different angle and orientations are being extracted. Unfortunately, there are some added background linear features and some artifacts in the background are being highlighted as well due to CLAHE and also the size of structuring elements. Background removal process is used to reduce these artifacts.

Due to the limitation of morphological operations, active contour model or snake is used to obtain vessel from noisy background. The created initial contour plays an important role because the structure of the contour will affect the quality and efficiency of the segmentation process. The number of iterations has set to 1000 because it created a high accuracy result while maintaining a reasonable computational time which is about 4 minutes. Besides, the performance of snake especially for accurate segmentation at vessel border in low and inconsistent contrast images is moderate high. The result can be improved by reducing the over segmentation to artifacts from pre-processing stage.

20 Images from Drive database are used to measure the performance of the developed algorithm and to compare with the performance with other published methods.

Performance analysis shows that the accuracy, sensitivity and specificity of the algorithm achieved a mean of 92.62%, 93.08% and 81.38% respectively. Given that the range of true positive fraction is slightly low, the algorithm is found slightly unreliable in detecting and reconstructing retinal vasculature in colour fundus images. If based on the accuracy parameter, the developed algorithm is comparable to other methods such as pixel classification [50] and method by Zana [52].

For detection of small vessels, false negative parameter is a better performance parameter to be used. The smaller the false negative is the more thin vessels are being segmented as under segmentation mainly occurs at thin vessels. The developed algorithm achieved low FN at mean 5.85% which shows that it is reliable in detecting and reconstructing thin vessels. The accuracy of the binary map of retinal vasculature is important to assist future analysis such as analysis of foveal avascular zone [5], tortuosity and etc.

The created Graphic User Interface (GUI) has eased the user of this algorithm in observing the result for each stage of the algorithm. It has also simplified the process of performance measurement and displayed the results of performance parameters accordingly in the table in the GUI.

## **CHAPTER 5**

### **CONCLUSION AND RECOMMENDATION**

#### **5.1 Conclusion**

As a conclusion, segmentation of retinal vasculature is very important because an accurate segmented retinal vessel will lead to higher accuracy of many other types of feature extraction algorithm such as analysis of FAZ. The high accuracy of these algorithms is very important to diagnose diseases such as diabetic retinopathy, hypertension, and etc. As a result, an active contour model, snake is used to obtained a good segmented blood vessel. During vessel detection phase, Contrast Limited Adaptive Histogram Equalization (CLAHE), sum of bottom hat morphological operation are used to enhance the contrast of the retinal image and detect the blood vessel from the image. The output is then used by Active Contour model for vessel segmentation. The result of these processes is an image of extracted retinal vessels with high intensity level and well contrasted with its background. The performance of the developed algorithm is then analyzed and compare with other proposed method. The algorithm is proven to be reliable in extracting small vessels. However, the algorithm need to be fine tune to avoid over segmentation due to it high value of FP fraction.

#### **5.2 Recommendation**

The project can be enhanced in the future based on the following recommendations:

- i. Another contrast enhancement method should be researched and replaced CLAHE in order to reduce the number of artifacts and produce better results for segmentation.
- ii. Another noise removal method should be researched in order to remove noise more efficiently compare to background removal.
- iii. The active contour model should be modified to perform better in detecting blood vessel while reduce the amount of over segmentation.

## REFERENCES

- [1] T O Lim, Z Morad., "Prevalence, Awareness, Treatment and Control of Hypertension in the Malaysian Adult Population: Results from the National Health and Morbidity Survey 1996 ." Singapore Med Journal, 2004, pp. 20-27.
- [2] , *Screening for Diabetic Retinopathy*. Kuala Lumpur : Malaysia Ministry of Health, 1996.
- [3] *Disease Center: Wrong Diagnosis, Statistic by Country for Type 2 Diabetes*. 2004.
- [4] Kanski, Jack J., *Clinical Ophthalmology: A Systematic Approach*. 6th ed. s.l. : Butterworth-Heinemann, 2007.
- [5] Ahmad Fadzil H.H., Lila Iznita I., *A non-invasive method for analyzing the retinal for ocular manifested diseases*. Malaysia, September 2008.
- [6] , High Blood Pressure (Hypertension) Overview, Causes. *Cardiology Channel*. [Online] 21 January 2008. [Cited: 8 August 2008.] <http://www.cardiologychannel.com/hypertension/index.shtml>.
- [7] Donald VIDT, MD., Disease Management Project. *Cleveland Clinic*. [Online] 12 January 2004. [Cited: 10 August 2008.] <http://www.clevelandclinicmeded.com/medicalpubs/diseasemanagement/nephrology/hypertension/hyptables.htm>.
- [8] , Hypertension. *My Health Portal*. [Online] 25 January 2006. [Cited: 6 August 2008.] [http://www.myhealth.gov.my/myhealth/eng/wargaemas\\_content.jsp?lang=wargaemas&sub=0&bhs=eng&storyid=1132190055013](http://www.myhealth.gov.my/myhealth/eng/wargaemas_content.jsp?lang=wargaemas&sub=0&bhs=eng&storyid=1132190055013).
- [9] Giansanti Roberto, Boemi Massino, Furnelli Paolo, Passerini Giorgio, Zingaretti Primo., "Quantitative analysis of retinal changes in hypertension." *Medical Image* 1995, 1995, pp. 548-556.
- [10] , Diabetic Retinopathy. *Pantheo Eye Centre*. [Online] 2008. [Cited: 10 August 2008.] <http://www.pantheo.com/patientinformation.php?pamphlet=3>.
- [11] Hypertensive Retinopathy. *Medline Plus*. [Online] 2 September 2008. [Cited: 28 August 2008.] <http://www.nlm.nih.gov/medlineplus/ency/imagepages/19530.htm>.
- [12] Retinal vessel narrowing predicts severe hypertension.(News Review). *High Beam Research*. [Online] 15 September 2004. [Cited: 3 August 2008.] <http://www.highbeam.com/doc/1G1-122622653.html>.

- [13] Hypertensive Retinopathy. [Online] 2006. [Cited: 8 August 2008.] <http://www.revoptom.com/handbook/SECT41b.HTM>.
- [14] Ophthalmoscopy. *studentmess*. [Online] 2008. [Cited: 30 August 2008.] <http://www.studentmess.com/index.php?p=163>.
- [15] Hypertension. *Cardiology explained*. [Online] 2004. [Cited: 28 August 2008.] <http://www.ncbi.nlm.nih.gov/bookshelf/br.fcgi?book=cardio&part=A379>.
- [16] Ocular Fundus Imaging. *Ophthalmic Photographers' Society*. [Online] 2008. [Cited: 11 August 2008.] <http://www.opsweb.org/OpPhoto/Fundus/index.html>.
- [17] Monochromatic Fundus Imaging. *Ophthalmic Photographers' Society*. [Online] 2008. [Cited: 11 August 2008.] <http://www.opsweb.org/OpPhoto/Fundus/Mono/MonoChrm.html>.
- [18] Nearest Neighbour Interpolation. [Online] 26 September 2006. [Cited: 2 September 2008.] <http://iria.pku.edu.cn/~jiangm/courses/dip/html/node67.html>.
- [19] Digital Image Interpolation. *cambridgeincolour*. [Online] 2008. [Cited: 31 August 2008.] <http://www.cambridgeincolour.com/tutorials/image-interpolation.htm>.
- [20] Bi-Cubic Interpolation. [Online] 26 September 2006. [Cited: 2 September 2008.] <http://iria.pku.edu.cn/~jiangm/courses/dip/html/node69.html>.
- [21] Mean Filter. *Image Metrology*. [Online] 2007. [Cited: 3 September 2008.] [http://www.imagemet.com/WebHelp/spip.htm#hid\\_filters\\_smoothing\\_mean.htm](http://www.imagemet.com/WebHelp/spip.htm#hid_filters_smoothing_mean.htm).
- [22] Rafael C. Gonzalez; Richard E. Woods., *Digital Image Processing*. New Jersey : Prentice-Hall, 2002.
- [23] Izhar, Lila iznita., *Analysis of Retinal Vasculature and Foveal Avascular Zone for Grading of Diabetic Retinopathy*. Tronoh : University Teknologi PETRONAS, 2006.
- [24] R. Fisher, S. Perkins, A. Walker and E. Wolfart., Contrast Stretching. [Online] 2003. [Cited: 3 September 2008.] <http://homepages.inf.ed.ac.uk/rbf/HIPR2/stretch.htm>.
- [25] —. Histogram Equalization. [Online] 2003. [Cited: 3 September 2008.] <http://homepages.inf.ed.ac.uk/rbf/HIPR2/histeq.htm>.
- [26] , adapthisteq. *The Math Works*. [Online] 2008. [Cited: 4 September 2008.] <http://www.mathworks.com/access/helpdesk/help/toolbox/images/index.html?/access/helpdesk/help/toolbox/images/adapthisteq.html&http://www.mathworks.com/cgi-bin/texis/webinator/search/>.
- [27] Benson Shu Yan Lam, Hong Yan., "A Novel Vessel Segmentation Algorithm for Pathological Retinal Images Basee on the Divergence of Vector Fields." s.l. : IEEE Transactions on Medical Imaging, February 2008, Issue 2, Vol. 27.

- [28] J.J.Staal, M.D.Abramoff, M.Niemeijer, M.A.Viergever, B.van Ginneken., "Ridge based vessel segmentation in colour images of the retinal." IEEE Transactions on Medical Imaging : s.n., 2004. Vol. 23, pp. 501-509.
- [29] Adam Hoover, Valentina Louznetsova, Michael Goldbaum., "Locating Blood vessels in Retinal Vessels in Retinal Images by Piecewise Threshold Probing of a Matched Filter Response." IEEE Transactions on Medical Imaging, March 2000, Issue 3, Vol. 19, pp. 203-210.
- [30] S. Chaundhuri, S. Chatterjee, N. Katz, M. Nelson, M. Goldbaum., "Detection of blood vessels in retinal images using two-dimensional matched filters." IEEE Trans. Med. Imag., Sept 1989, Vol. 8, pp. 263-269.
- [31] , Morphological Operation. *weizmann*. [Online] 2008. [Cited: 4 September 2008.] <http://www.weizmann.ac.il/matlab/toolbox/images/morph.html>.
- [32] Dilation and Erosion. *weizmann*. [Online] 2008. [Cited: 4 September 2008.] <http://www.weizmann.ac.il/matlab/toolbox/images/morph3.html#12508>.
- [33] R. Fisher, S. Perkins, A. Walker and E. Wolfart., Opening. [Online] 2003. [Cited: 5 September 2008.] <http://homepages.inf.ed.ac.uk/rbf/HIPR2/index.htm>.
- [34] L. Espona, M.J.Carreira., "Retinal Vessel Tree Segmentation using a Deformable Contour Model." s.l. : IEEE, 2008.
- [35] Milan Sonka, Vaclav Hlavac, Roger Boyle., *Image Processing, Analysis, and Machine Vision*. 3rd Edition. Toronto : Thomson Learning, 2008.
- [36] Berger M.O., Mohr R., "Towards autonomy on active contour models." Atlantic City : IEEE, 1990. 10th International Conference on Pattern Recognition. pp. 847-851.
- [37] L.D., Cohen., "On active contour models and balloons." s.l. : CVGIP-Image Understanding, 1991, Issue 2, Vol. 53, pp. 211-218.
- [38] G Hamarneh, T Gustavsson., "Combining Snakes and Active Shape Models for Segmenting the HUMAN Ventricle in Echocardiographic Images." s.l. : IEEE Computers in Cardiology , 2000, Vol. 27.
- [39] Xin U Liu, Mark S Nixon., "Water Flow Based Vessel Detection in Retinal Images." s.l. : VIE 2006, 2006, pp. 345-350.
- [40] Xin U Liu, MARK S Nixon., "Medical Image Segmentation by Water Flow."
- [41] Chunming Li, Chenyang Xu, Changfeng Gui, Martin D. Fox., "Level Set Evolution without Re-initialization: A New Variational Formulation." Proceedings of the 2005 IEEE Computer Society Conference on Computer Vision and Pattern Recognition.
- [42] S. Osher, J.A. Sethian., "Fronts propagating with crvature-dependent speed: algorithm based on Hamilton-Jacobi formulation." s.l. : J. Comp. Phys., 1988, Vol. 79, pp. 12-49.

- [43] S. Tamura, Y. Okamoto, and K. Yanashima., "Zero-crossing interval correction in tracing eye-fundus blood vessels." *Pattern Recognition* , Issue 3, Vol. 21, pp. 227-233.
- [44] Y. Sun., "Automated identification of vessel contours in coronary arteriograms by an adaptive tracking algorithm." *IEEE Transaction on Medical Imaging*, March 1989, Vol. 8, pp. 78-88.
- [45] Rosfarizan., *Biomedical Image Processing for Breast Cancer*. Perak : Universiti Teknologi PETRONAS, 2008.
- [46] C. Sinthanayothin, J.F. Boyce, T.H. Williamson, H.L. Cook, E. mensah, S. Lai, D. Usher., "Automated detection of diabetic retinopathy on digital fundus images." *Diabetic Med.*, 2002, Issue 2, Vol. 19, pp. 105-112.
- [47] Tuan D. Pham, Dat T. Tran, Marianne Brown, R. Lee Kennedy., "Image Segmentation of Retinal Vessels by Fuzzy Models." *Hong Kong : 2005 International Symposium on Intelligent Signal Processing and Communication Systems*, 2005. pp. 541-544.
- [48] Xuemin Wang, Hongbao Cao, Jie Zhang., "Analysis of Retinal Images Associated with Hypertension and Diabetes." *Shanghai : IEEE, 2005. Engineering in Medicine and Biology 27th Annual Conference*. pp. 6407-6410.
- [49] Peng Zhou, Mingshi Wang, Hongbao Cao., "Research on Features of Retinal Images Associated with Hypertension and Diabetes." *Shanghai : IEEE, 2005. Engineering in Medicine and Biology 27th Annual Conference*. pp. 6415-6417.
- [50] M. Niemeijer, J.J. Staal, B. van Ginneken, M. Loog, M.D. Abramoff., "Comparative study of retinal vessel segmentation methods on a new publicly available database." [ed.] M. Sonka J. Michael Fitzpatrick. *SPIE Medical Imaging*, s.l. : SPIE, 2004, Vol. 5370, pp. 648-656.
- [51] Tony F. Chan, Luminita A. Vese., "Active Contours Without Edges." s.l. : IEEE *Transactions on Image Processing*, 2001, Issue 2, Vol. 10, pp. 266-276.
- [52] Zana F., Klein J.C., "segmentation of vessel like patterns using morphology and curvature evaluation." s.l. : IEEE *Transactions on Image Processing*, 2001, Issue 7, Vol. 10, pp. 1010-1019.
- [53] Jiang X. , Mojon D., "Adaptive local thresholding by verification-based multithreshold probing with application to vessel detection in retinal image." s.l. : IEEE *Transactions on Pattern Analysis and Machine Intelligence*, 1993, Issue 1, Vol. 25, pp. 131-137.
- [54] Martinez-Perez M., Hughes A., Stanton A., Thom S., Bharath A., Parker K., "Scale-space Analysis for the Characterization of Retinal Blood Vessels." s.l. : *Medical Image Computing and Computer Assisted Intervention - MICCAI'99*, 1999. pp. 90-97.
- [55] Non-Mydriatic Fundus Camera. *Kowa*. [Online] 2005. [Cited: 3 August 2008.] <http://www.kowa.co.jp/e-life/products/fc/nonmyd7.htm>.

[56] KOWA nonmyd 7 / VK-2 Digital Imaging System. *medcompare*. [Online] 2008. [Cited: 1 August 2008.] <http://www.medcompare.com/details/10784/KOWA-nonmyd-7--VK-2-Digital-Imaging-System.html>.

[57] Cristian Perra, Maria Petrou, Daniele D. Giusto., "Retinal image Segmentation by Watersheds." s.l. : IAPR Workshop on Machine Vision Applications, 2000. pp. 315-318.

[58] C. Alonso-Montes, D.L.Vilarino, P.Dudek and M.G.Penedo., "Fast Retinal Vessel Tree Extraction: A Pixel Parallel Approach." s.l. : International Journal of Circuit Theory and Applications, 2008, Vol. 36, pp. 641-651.

[59] Michal Sofka, Charles V. Stewart., "Retinal Vessel Centerline Extraction Using Multiscale Matched Filters, Confidence and Edge Measures." s.l. : IEEE Transactions on Medical Imaging, December 2006, Issue 12, Vol. 25, pp. 1531-1546.

[60] Huiqi Li, Opas Chutatape., "Automated Teature Extraction in Colour Retinal IMages by a Model based Approach." s.l. : IEEE Transactions on Biomedical Engineering, February 2004, Issue 2, Vol. 51, pp. 246-254.

[61] Qin Li, Jane You, Lei Zhang, David Zhang., "A New Approach to Automated Retinal Vessel Segmentation Using Multiscale Analysis." s.l. : The 18th International Conference on Pattern Recognition (ICPR'06), 2006.

[62] Matei MANCAS, Bernard GOSSELIN, Benoit MACQ., "Segmentation Using Region Growing Thresholding."

[63] Thitiporn Chanwimaluang, Guoliang Fan ., "An Efficient Blood Vessel Detection Algorithm for Retinal Images using Local Entropy Thresholding." Oklahoma : s.n.

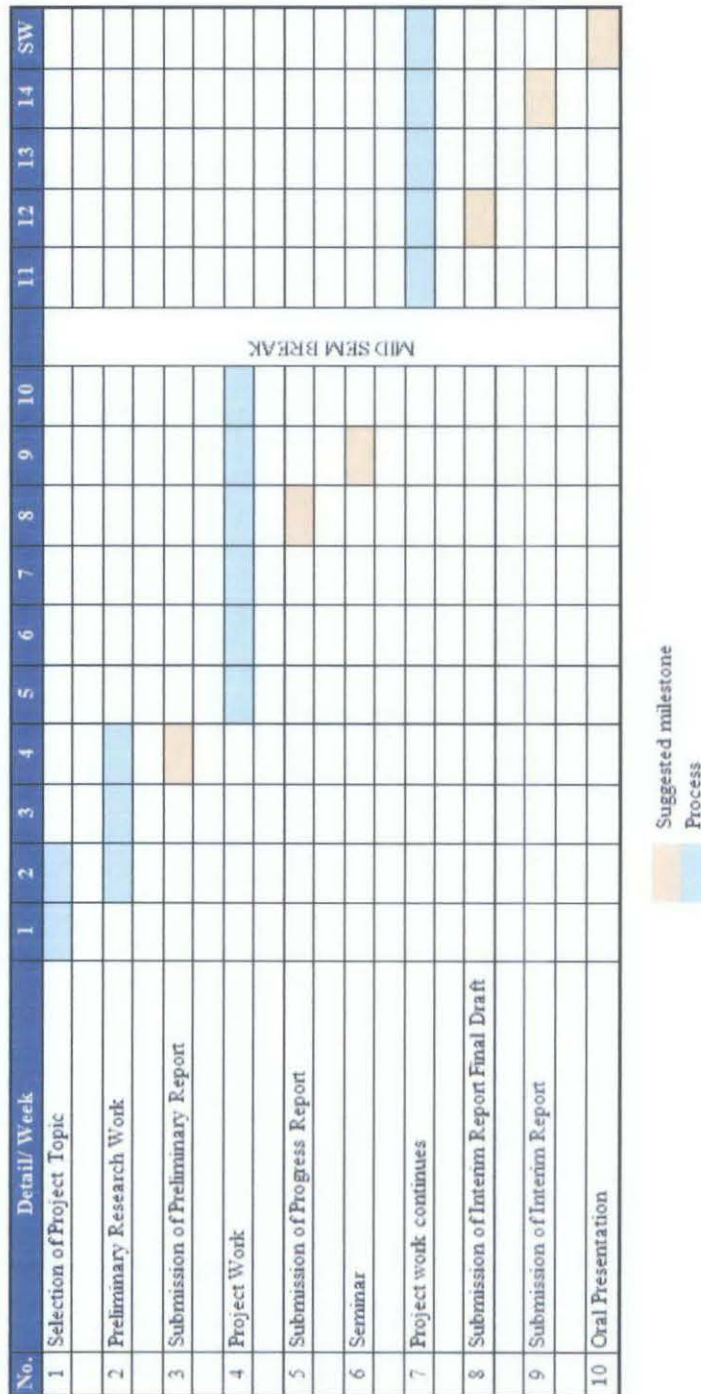
[64] Samuel H. Chang, Leiguang Gong, Maoqing Li, Xiaoying Hu, Jingwen Yan., "Small Retinal Vessel Extraction Using Modified Canny Edge Detection." s.l. : ICALIP2008, 2008. pp. 1255-1259.

## APPENDICES

### APPENDIX A1

#### Gantt Chart of the Final Year Project (1<sup>st</sup> Semester)

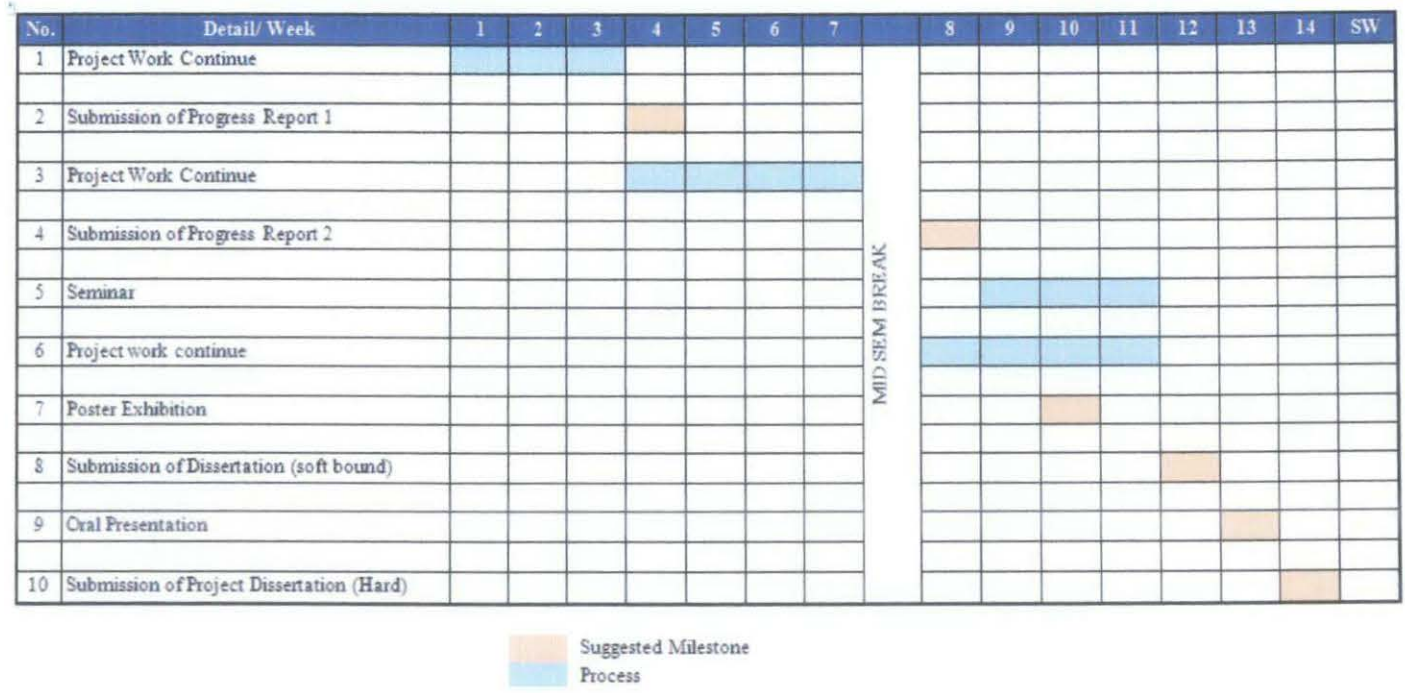
Milestone of First Semester in Final Year Project



APPENDIX A2

Gantt Chart of the Final Year Project (2<sup>nd</sup> Semester)

Milestone of Second Semester in Final Year Project



## APPENDIX B

### Information of the Fundus Camera

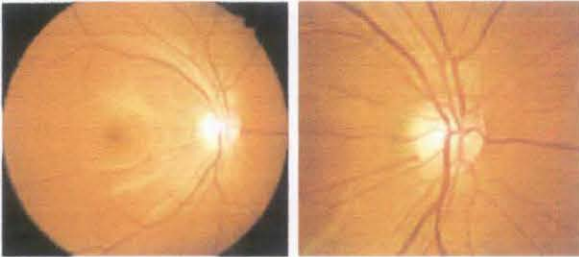
Non-Mydriatic Fundus Camera

**Kowa** *nonmyd*™ 7



The nonmyd 7, an easy-to-use fundus camera with the capability of 10 megapixel high-resolution photography. Sharper, clearer images will guarantee outstanding performance in clinic scenes.

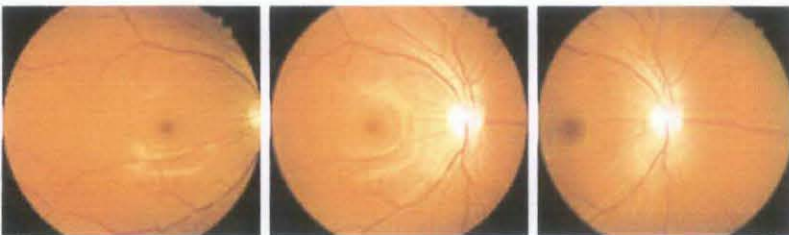
2 optical angles



45°

20°

3 internal fixation targets



Temporal

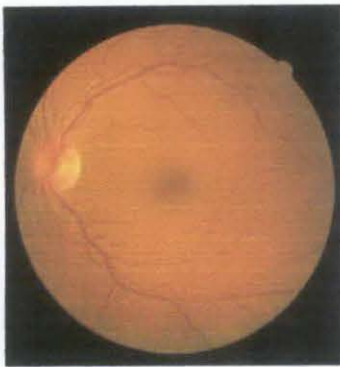
Central

Nasal

## General Information

<b>Vendor</b>	<b>Kowa Optimed, Inc</b>
<b>Item</b>	<b>KOWA nonmyd 7 / VK-2 Digital Imaging System</b> <ul style="list-style-type: none"><li>• Digital 10 Mega-Pixels External Integrated Camera Back</li><li>• Nonmyd Color 45 degree / 20 degree Optical Magnification</li><li>• Small Pupil Mode</li><li>• Multiple Step Flash</li><li>• Focusing/Alignment Dots</li><li>• Easy to Operate</li><li>• VK-2 Digital Imaging Software</li></ul>
<b>Features</b>	
<b>Approval</b>	Worldwide
<b>Type</b>	Fundus camera
<b>Product Number</b>	KOWA nonmyd 7
<b>Working Distance</b>	40mm (between objective lens and cornea)
<b>Photographic Angles</b>	20° 35° and 50°
<b>Film</b>	35mm Color Film ISO 100 Fluorescein ISO 400 (3 times sensitized) Polaroid Film ISO 600 (for color)
<b>Image Magnification/Resolution</b>	1.9x, 2.7x & 4.6x
<b>Digital Imaging (Y/N)</b>	Yes, VK-2 Digital Imaging System
<b>Digital Resolution</b>	10 Mega-Pixels

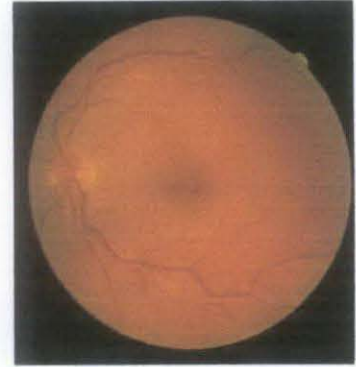
**APPENDIX C**  
**IMAGES FROM DRIVE DATABASE [50]**



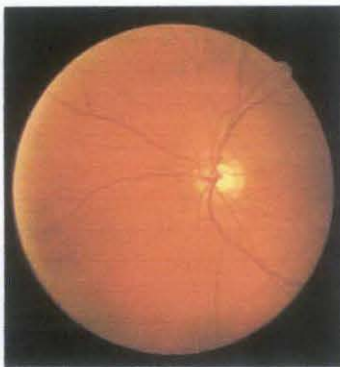
01\_TEST



02\_TEST



03\_TEST



04\_TEST



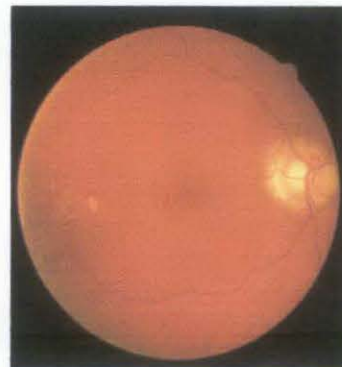
05\_TEST



06\_TEST



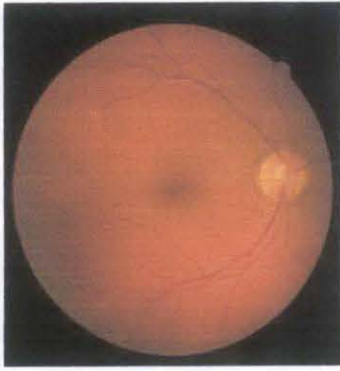
07\_TEST



08\_TEST



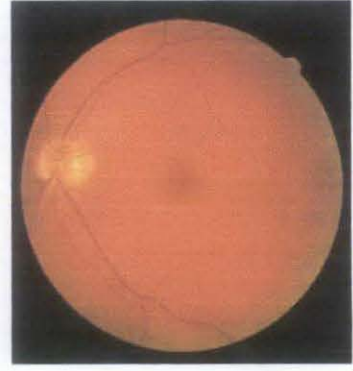
09\_TEST



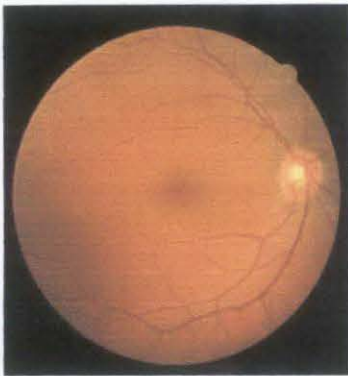
10\_TEST



11\_TEST



12\_TEST



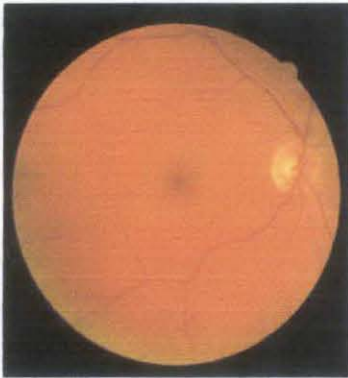
13\_TEST



14\_TEST



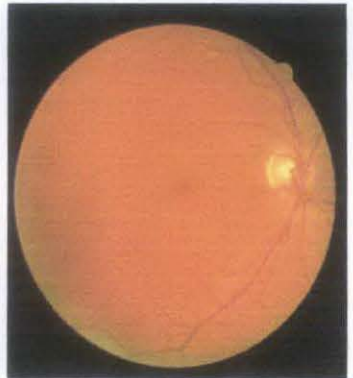
15\_TEST



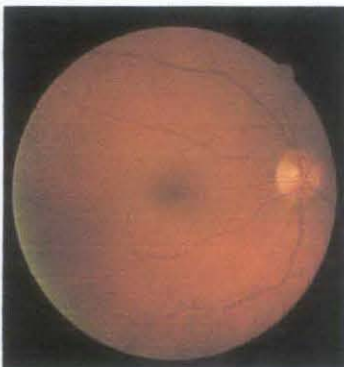
16\_TEST



17\_TEST



18\_TEST



19\_TEST



20\_TEST

## APPENDIX D PROJECT SOURCE CODE

```
%%Graphic User Interface for Final Year Project

function varargout = FYPgui(varargin)
% FYPGUI M-file for FYPgui.fig
%   FYPGUI, by itself, creates a new FYPGUI or raises the existing
%   singleton*.
%
%   H = FYPGUI returns the handle to a new FYPGUI or the handle to
%   the existing singleton*.
%
%   FYPGUI('CALLBACK',hObject,eventData,handles,...) calls the local
%   function named CALLBACK in FYPGUI.M with the given input arguments.
%
%   FYPGUI('Property','Value',...) creates a new FYPGUI or raises the
%   existing singleton*. Starting from the left, property value pairs
are
%   applied to the GUI before FYPgui_OpeningFunction gets called. An
%   unrecognized property name or invalid value makes property
application
%   stop. All inputs are passed to FYPgui_OpeningFcn via varargin.
%
%   *See GUI Options on GUIDE's Tools menu. Choose "GUI allows only one
%   instance to run (singleton)".
%
% See also: GUIDE, GUIDATA, GUIHANDLES

% Edit the above text to modify the response to help FYPgui

% Last Modified by GUIDE v2.5 13-Apr-2009 23:02:32

% Begin initialization code - DO NOT EDIT
gui_Singleton = 1;
gui_State = struct('gui_Name',       mfilename, ...
                  'gui_Singleton',  gui_Singleton, ...
                  'gui_OpeningFcn', @FYPgui_OpeningFcn, ...
                  'gui_OutputFcn',  @FYPgui_OutputFcn, ...
                  'gui_LayoutFcn',  [], ...
                  'gui_Callback',   []);
if nargin && ischar(varargin{1})
    gui_State.gui_Callback = str2func(varargin{1});
end

if nargout
    [varargout{1:nargout}] = gui_mainfcn(gui_State, varargin{:});
else
    gui_mainfcn(gui_State, varargin{:});
end
```

```

end
% End initialization code - DO NOT EDIT

% --- Executes just before FYPgui is made visible.
function FYPgui_OpeningFcn(hObject, eventdata, handles, varargin)
% This function has no output args, see OutputFcn.
% hObject    handle to figure
% eventdata  reserved - to be defined in a future version of MATLAB
% handles    structure with handles and user data (see GUIDATA)
% varargin   command line arguments to FYPgui (see VARARGIN)

% Choose default command line output for FYPgui
handles.output = hObject;

% Update handles structure
guidata(hObject, handles);

% UIWAIT makes FYPgui wait for user response (see UIRESUME)
% uiwait(handles.figure1);

% --- Outputs from this function are returned to the command line.
function varargout = FYPgui_OutputFcn(hObject, eventdata, handles)
% varargout  cell array for returning output args (see VARARGOUT);
% hObject    handle to figure
% eventdata  reserved - to be defined in a future version of MATLAB
% handles    structure with handles and user data (see GUIDATA)

% Get default command line output from handles structure
varargout{1} = handles.output;

% --- Executes on button press in LoadImage.
function LoadImage_Callback(hObject, eventdata, handles)
% hObject    handle to LoadImage (see GCBO)
% eventdata  reserved - to be defined in a future version of MATLAB
% handles    structure with handles and user data (see GUIDATA)
axes(handles.axes1);
[FileName,PathName] = uigetfile('*..*','Select any RGB image');
y = [PathName,FileName];
img = imread(y);
imshow(img),title('Original Image');

% --- Executes on button press in LoadManual.
function LoadManual_Callback(hObject, eventdata, handles)
% hObject    handle to LoadManual (see GCBO)
% eventdata  reserved - to be defined in a future version of MATLAB
% handles    structure with handles and user data (see GUIDATA)
[FileName,PathName] = uigetfile('*..*','Select any RGB image');
y = [PathName,FileName];
I_a = imread(y);
axes(handles.axes9);

```

```

imshow(I_a),title('Manually Segmented Image');

% --- Executes on button press in LoadMask.
function LoadMask_Callback(hObject, eventdata, handles)
% hObject      handle to LoadMask (see GCBO)
% eventdata    reserved - to be defined in a future version of MATLAB
% handles      structure with handles and user data (see GUIDATA)
[FileName,PathName] = uigetfile('*.','Select any RGB image');
y = [PathName,FileName];
I_m = imread(y);
axes(handles.axes8);
imshow(I_m),title('Mask');

% --- Executes on button press in VDetection.
function VDetection_Callback(hObject, eventdata, handles)
% hObject      handle to Preprocessing (see GCBO)
% eventdata    reserved - to be defined in a future version of MATLAB
% handles      structure with handles and user data (see GUIDATA)

%get the green band of the retinal image
T=getimage(handles.axes1);
axes(handles.axes2);
G=T(:, :,2);
imshow(G),title('Green Band');

%enlarge the image
G2 = imresize(G,2,'bicubic');

%perform the median filtering
MED2 = medfilt2(G2,[4 4]);

%resize the result image
MED = imresize(MED2,0.5,'bicubic');

axes(handles.axes3);

%perform CLAHE
Gclahe = adapthisteq(MED);
imshow(Gclahe),title('After CLAHE');

%define the strel
se1 = strel('line',15,15);
se2 = strel('line',15,30);
se3 = strel('line',15,45);
se4 = strel('line',15,60);
se5 = strel('line',15,75);
se6 = strel('line',15,90);
se7 = strel('line',15,105);
se8 = strel('line',15,120);
se9 = strel('line',15,135);
se10 = strel('line',15,150);
se11 = strel('line',15,165);
se12 = strel('line',15,180);

%perform the sum of bottom hat morphological process

```

```

BT1=imbothat(Gclahe,se1);
BT2=imbothat(Gclahe,se2);
BT3=imbothat(Gclahe,se3);
BT4=imbothat(Gclahe,se4);
BT5=imbothat(Gclahe,se5);
BT6=imbothat(Gclahe,se6);
BT7=imbothat(Gclahe,se7);
BT8=imbothat(Gclahe,se8);
BT9=imbothat(Gclahe,se9);
BT10=imbothat(Gclahe,se10);
BT11=imbothat(Gclahe,se11);
BT12=imbothat(Gclahe,se12);
BTsum=BT1+BT2+BT3+BT4+BT5+BT6+BT7+BT8+BT9+BT10+BT11+BT12;
axes(handles.axes4);
imshow(BTsum),title('After Bottom-Hat');

%Background Removal
Back = imfilter(BTsum,fspecial('average',[40 40]));
Sub2 = imsubtract(BTsum, Back);
CS = imadjust(Sub2,[5/255 200/255]);
axes(handles.axes5);
imshow(CS),title('After Background Removal');

% --- Executes on button press in PerformanceParameter.
function PerformanceParameter_Callback(hObject, eventdata, handles)
% hObject      handle to PerformanceParameter (see GCBO)
% eventdata    reserved - to be defined in a future version of MATLAB
% handles      structure with handles and user data (see GUIDATA)

Image=getimage(handles.axes6);
I_a=getimage(handles.axes9);
I_m=getimage(handles.axes8);
output=FYPanalysis2(Image,I_a,I_m);

% Get the Handle for the TP Tag
TP = findobj(gcf,'Tag','TP');
% Set the string for the object TFinal
set(TP,'String',[num2str(output(2),'%.4f')])

% Get the Handle for the FP Tag
FP = findobj(gcf,'Tag','FP');
% Set the string for the object TFinal
set(FP,'String',[num2str(output(3),'%.4f')])

% Get the Handle for the TN Tag
TN = findobj(gcf,'Tag','TN');
% Set the string for the object TFinal
set(TN,'String',[num2str(output(4),'%.4f')])

% Get the Handle for the FN Tag
FN = findobj(gcf,'Tag','FN');
% Set the string for the object TFinal
set(FN,'String',[num2str(output(5),'%.4f')])

```

```

% Get the Handle for the SP Tag
SP = findobj(gcf,'Tag','SP');
% Set the string for the object TFinal
set(SP,'String',[num2str(output(6),'%.4f')])

% Get the Handle for the SE Tag
SE = findobj(gcf,'Tag','SE');
% Set the string for the object TFinal
set(SE,'String',[num2str(output(7),'%.4f')])

% Get the Handle for the ACU Tag
ACU = findobj(gcf,'Tag','ACU');
% Set the string for the object TFinal
set(ACU,'String',[num2str(output(1),'%.4f')])

function edit1_Callback(hObject, eventdata, handles)
% hObject      handle to edit1 (see GCBO)
% eventdata    reserved - to be defined in a future version of MATLAB
% handles      structure with handles and user data (see GUIDATA)

% Hints: get(hObject,'String') returns contents of edit1 as text
%         str2double(get(hObject,'String')) returns contents of edit1 as
a double

% --- Executes during object creation, after setting all properties.
function edit1_CreateFcn(hObject, eventdata, handles)
% hObject      handle to edit1 (see GCBO)
% eventdata    reserved - to be defined in a future version of MATLAB
% handles      empty - handles not created until after all CreateFcns
called

% Hint: edit controls usually have a white background on Windows.
%         See ISPC and COMPUTER.
if ispc && isequal(get(hObject,'BackgroundColor'),
get(0,'defaultUicontrolBackgroundColor'))
    set(hObject,'BackgroundColor','white');
end

% --- Executes on button press in Reset.
function Reset_Callback(hObject, eventdata, handles)
% hObject      handle to Reset (see GCBO)
% eventdata    reserved - to be defined in a future version of MATLAB
% handles      structure with handles and user data (see GUIDATA)

axes(handles.axes1);
cla;
axes(handles.axes2);
cla;
axes(handles.axes3);
cla;

```

```

axes(handles.axes4);
cla;
axes(handles.axes5);
cla;
axes(handles.axes6);
cla;
axes(handles.axes7);
cla;
axes(handles.axes8);
cla;
axes(handles.axes9);
cla;
% Get the Handle for the TP Tag
TP = findobj(gcf,'Tag','TP');
% Set the string for the object TFinal
set(TP,'String',[num2str(0,'%4f')])

% Get the Handle for the FP Tag
FP = findobj(gcf,'Tag','FP');
% Set the string for the object TFinal
set(FP,'String',[num2str(0,'%4f')])

% Get the Handle for the TN Tag
TN = findobj(gcf,'Tag','TN');
% Set the string for the object TFinal
set(TN,'String',[num2str(0,'%4f')])

% Get the Handle for the FN Tag
FN = findobj(gcf,'Tag','FN');
% Set the string for the object TFinal
set(FN,'String',[num2str(0,'%4f')])

% Get the Handle for the SP Tag
SP = findobj(gcf,'Tag','SP');
% Set the string for the object TFinal
set(SP,'String',[num2str(0,'%4f')])

% Get the Handle for the SE Tag
SE = findobj(gcf,'Tag','SE');
% Set the string for the object TFinal
set(SE,'String',[num2str(0,'%4f')])

% Get the Handle for the ACU Tag
ACU = findobj(gcf,'Tag','ACU');
% Set the string for the object TFinal
set(ACU,'String',[num2str(0,'%4f')])

% --- Executes on button press in VSegmentation.
function VSegmentation_Callback(hObject, eventdata, handles)
% hObject      handle to Segmentation (see GCBO)
% eventdata    reserved - to be defined in a future version of MATLAB
% handles      structure with handles and user data (see GUIDATA)

CS=getimage(handles.axes5);

```

```

axes(handles.axes7);
mask=FYPmask(CS);
imshow(mask),title('Initial Contour');
axes(handles.axes6);
Iteration = str2double(get(handles.Iteration,'String'));

% if no input from user, default no. of iteration is 1000
if isnan(Iteration)
    Iteration = 1000;
End

% perform image segmentation using active contour model
image=region_seg_demo(CS,mask,Iteration);

function Iteration_Callback(hObject, eventdata, handles)
% hObject    handle to Iteration (see GCBO)
% eventdata  reserved - to be defined in a future version of MATLAB
% handles    structure with handles and user data (see GUIDATA)

% Hints: get(hObject,'String') returns contents of Iteration as text
%        str2double(get(hObject,'String')) returns contents of
Iteration as a double
user_entry = str2double(get(hObject,'string'));
if isnan(user_entry)
    errordlg('You must enter a numeric value','Bad Input','modal')
end

% --- Executes during object creation, after setting all properties.
function Iteration_CreateFcn(hObject, eventdata, handles)
% hObject    handle to Iteration (see GCBO)
% eventdata  reserved - to be defined in a future version of MATLAB
% handles    empty - handles not created until after all CreateFcns
called

% Hint: edit controls usually have a white background on Windows.
%        See ISPC and COMPUTER.
if ispc && isequal(get(hObject,'BackgroundColor'),
get(0,'defaultUiControlBackgroundColor'))
    set(hObject,'BackgroundColor','white');
end

```

```

%-----
%-----
%-- AUXILIARY FUNCTIONS -----
%-----
%-----

```

```

%%%%%%%%%%%%%%%%%%%%%%%%%%%%%%%%%%%%%%%%%%%%%%%%%%%%%%%%%%%%%%%%%%%%%%%%
%
% create an initial contour based on original image's size
%
% output = mask(I)
%
% Input:    I= 2D image
%
% example:  I=imread('sample.tif');
%           mask = mask(I);
%
%%%%%%%%%%%%%%%%%%%%%%%%%%%%%%%%%%%%%%%%%%%%%%%%%%%%%%%%%%%%%%%%%%%%%%%%

```

```
function output=mask(I)
```

```
[m,n] = size(I);
```

```
%5 stripes of the initial contour
```

```

j = zeros(size(I,1),size(I,2));
j(70:m-70,50:50+20) = 1;
p= zeros(size(I,1),size(I,2));
p(70:m-70,70+(n-200)/4:70+(n-200)/4+20) = 1;
k= zeros(size(I,1),size(I,2));
k(70:m-70,70+2*(n-200)/4+20:70+2*(n-200)/4+20+20) = 1;
l= zeros(size(I,1),size(I,2));
l(70:m-70,70+3*(n-200)/4+40:70+3*(n-200)/4+40+20) = 1;
o = zeros(size(I,1),size(I,2));
o(70:m-70,n-70:n-70+20) = 1;

```

```

m=j|p|k|l|o;
output=m;

```

```

%#####
%
% Active Contours Model (Snake)- Modelling
%
% output=region_seg_demo(I,m,iteration)
%
% Inputs:  I= 2D Image after Vessel Detection
%          m= mask as initial contour (can be generated using FYPmask.m
%          iteration= number of iterations
%
% Example:
% I=imread('image.tif');
% m=FYPmask(I);
% itx=500;
% output=region_seg_demo(I, m, its)
%
%#####

```

```

function output=region_seg_demo(I,m,iteration)

I = imresize(I,.5); % make image smaller for fast computation
m = imresize(m,.5);

title('Segmentation');
seg = region_seg(I, m, iteration); % Run vessel segmentation

seg2=imresize(seg,2); % resize back to original size

output=seg2;

imshow(seg2); title('After Segmentation');

```

```

% %%%%%%%%%%%%%%%%%%%%%%%%%%%%%%%%%%%%%%%%%%%%%%%%%%%%%%%%%%
%
% Vessel Segmentation by Active Contour Model (Snake)
%
% seg = region_seg(I,init_mask,max_its,alpha,display)
%
% Inputs: I          2D image
%         init_mask  Initialization (1 = foreground, 0 = bg)
%         max_its    Number of iterations to run segmentation for
%         alpha      (optional) Weight of smoothing term
%                   higher = smoother.  default = 0.2
%         display    (optional) displays intermediate outputs
%                   default = true
%
% Outputs: seg       Final segmentation mask (1=fg, 0=bg)
%
%
% Example:
% img = imread('tire.tif');
% m = zeros(size(img));
% m(33:33+117,44:44+128) = 1;
% seg = region_seg(img,m,500);
%
% %%%%%%%%%%%%%%%%%%%%%%%%%%%%%%%%%%%%%%%%%%%%%%%%%%%%%%%%%%

```

```

function seg = region_seg(I,init_mask,max_its,alpha,display)

%-- default value for parameter alpha is .1
if(~exist('alpha','var'))
    alpha = .2;
end

%-- default behavior is to display intermediate outputs
if(~exist('display','var'))
    display = true;
end

%-- ensures image is 2D double matrix
I = im2graydouble(I);

%-- Create a signed distance map (SDF) from mask
phi = mask2phi(init_mask);

%--main loop
for its = 1:max_its    % Note: no automatic convergence test

    idx = find(phi <= 1.2 & phi >= -1.2);    %get the curve's narrow band

    %-- find interior and exterior mean
    upts = find(phi<=0);    % interior points
    vpts = find(phi>0);    % exterior points
    u = sum(I(upts))/(length(upts)+eps); % interior mean
    v = sum(I(vpts))/(length(vpts)+eps); % exterior mean

    F = (I(idx)-u).^2-(I(idx)-v).^2;    % force from image information

```

```

    curvature = get_curvature(phi,idx); % force from curvature penalty

    % gradient descent to minimize energy
    dphidt = F./max(abs(F)) + alpha*curvature;

    %-- maintain the CFL condition
    dt = .45/(max(dphidt)+eps);

    %-- evolve the curve
    phi(idx) = phi(idx) + dt.*dphidt;

    %-- Keep SDF smooth
    phi = sussman(phi, .5);

    %-- intermediate output
    if((display>0)&&(mod(its,20) == 0))
        showCurveAndPhi(I,phi,its);
    end
end

%-- final output
if(display)
    showCurveAndPhi(I,phi,its);
end

%-- make mask from SDF
seg = phi<=0; %-- Get mask from levelset

```

#### %Sub Functions

```

%-- Displays the image with curve superimposed
function showCurveAndPhi(I, phi, i)
    imshow(I,'initialmagnification',200,'displayrange',[0 255]); hold on;
    contour(phi, [0 0], 'g','LineWidth',4);
    contour(phi, [0 0], 'k','LineWidth',2);
    hold off; title([num2str(i) ' Iterations']); drawnow;

```

```

%-- converts a mask to a SDF
function phi = mask2phi(init_a)
    phi=bwdist(init_a)-bwdist(1-init_a)+im2double(init_a)-.5;

```

```

%-- compute curvature along SDF
function curvature = get_curvature(phi,idx)
    [dimy, dimx] = size(phi);
    [y x] = ind2sub([dimy,dimx],idx); % get subscripts

    %-- get subscripts of neighbors
    yml = y-1; xml = x-1; ypl = y+1; xpl = x+1;

    %-- bounds checking
    yml(yml<1) = 1; xml(xml<1) = 1;
    ypl(ypl>dimy)=dimy; xpl(xpl>dimx) = dimx;

```

```

%-- get indexes for 8 neighbors
idup = sub2ind(size(phi), yp1, x);
iddn = sub2ind(size(phi), yml, x);
idlt = sub2ind(size(phi), y, xml);
idrt = sub2ind(size(phi), y, xp1);
idul = sub2ind(size(phi), yp1, xml);
idur = sub2ind(size(phi), yp1, xp1);
iddl = sub2ind(size(phi), yml, xml);
idrr = sub2ind(size(phi), yml, xp1);

%-- get central derivatives of SDF at x,y
phi_x = -phi(idlt)+phi(idrt);
phi_y = -phi(iddn)+phi(idup);
phi_xx = phi(idlt)-2*phi(idx)+phi(idrt);
phi_yy = phi(iddn)-2*phi(idy)+phi(idup);
phi_xy = -0.25*phi(iddl)-0.25*phi(idur)...
         +0.25*phi(idrr)+0.25*phi(idul);
phi_x2 = phi_x.^2;
phi_y2 = phi_y.^2;

%-- compute curvature (Kappa)
curvature = ((phi_x2.*phi_yy + phi_y2.*phi_xx -
2*phi_x.*phi_y.*phi_xy)./...
            (phi_x2 + phi_y2 +eps).^(3/2)).*(phi_x2 + phi_y2).^(1/2);

%-- Converts image to one channel (grayscale) double
function img = im2graydouble(img)
[dimy, dimx, c] = size(img);
if(isfloat(img)) % image is a double
    if(c==3)
        img = rgb2gray(uint8(img));
    end
else % image is a int
    if(c==3)
        img = rgb2gray(img);
    end
    img = double(img);
end

%-- level set re-initialization by the sussman method
function D = sussman(D, dt)
% forward/backward differences
a = D - shiftR(D); % backward
b = shiftL(D) - D; % forward
c = D - shiftD(D); % backward
d = shiftU(D) - D; % forward

a_p = a; a_n = a; % a+ and a-
b_p = b; b_n = b;
c_p = c; c_n = c;
d_p = d; d_n = d;

a_p(a < 0) = 0;
a_n(a > 0) = 0;
b_p(b < 0) = 0;
b_n(b > 0) = 0;

```

```

c_p(c < 0) = 0;
c_n(c > 0) = 0;
d_p(d < 0) = 0;
d_n(d > 0) = 0;

dD = zeros(size(D));
D_neg_ind = find(D < 0);
D_pos_ind = find(D > 0);
dD(D_pos_ind) = sqrt(max(a_p(D_pos_ind).^2, b_n(D_pos_ind).^2) ...
    + max(c_p(D_pos_ind).^2, d_n(D_pos_ind).^2)) - 1;
dD(D_neg_ind) = sqrt(max(a_n(D_neg_ind).^2, b_p(D_neg_ind).^2) ...
    + max(c_n(D_neg_ind).^2, d_p(D_neg_ind).^2)) - 1;

D = D - dt .* sussman_sign(D) .* dD;

%-- whole matrix derivatives
function shift = shiftD(M)
    shift = shiftR(M')';

function shift = shiftL(M)
    shift = [ M(:,2:size(M,2)) M(:,size(M,2)) ];

function shift = shiftR(M)
    shift = [ M(:,1) M(:,1:size(M,2)-1) ];

function shift = shiftU(M)
    shift = shiftL(M')';

function S = sussman_sign(D)
    S = D ./ sqrt(D.^2 + 1);

```

```

%%%%%%%%%%%%%%%%%%%%%%%%%%%%%%%%%%%%%%%%%%%%%%%%%%%%%%%%%%%%%%%%%%%%%%%%
%
% Performance Analysis
%
% output=FYPanalysis2(image, I_a, I_m)
%
% Inputs:  image = 2D retinal segmented vessel for analysis
%          I_a   = hand labelled image
%          I_m   = mask for the retinal image
%
% Example:
%   I       =imread('image.tif');
%   label   =imread('labell.tif');
%   mask    =imread('mask.tif');
%   output=FYPanalysis(I, label, mask);
%
%%%%%%%%%%%%%%%%%%%%%%%%%%%%%%%%%%%%%%%%%%%%%%%%%%%%%%%%%%%%%%%%%%%%%%%%

```

```
function output=FYPanalysis2(image,I_a,I_m)
```

```
bw_a = im2bw(I_a,0.4);
```

```
%%Vessels segmented by developed algorithm
```

```
I_d = image;
```

```
bw_d = im2bw(I_d,0.4);
```

```
%%FOV mask
```

```
area = bwarea(I_m);
```

```
im = I_d;
```

```
H = size(im, 1);      % image height
```

```
W = size(im, 2);      %image width
```

```
Outside = ((H*W)-area);
```

```
%%Total pixel of hand-labeled vessels
```

```
V_a = 0;
```

```
for i=1:H
```

```
    for j=1:W
```

```
        if bw_a(i,j) ==1;
```

```
            V_a = V_a+1;
```

```
        end
```

```
    end
```

```
end
```

```
V_a;
```

```
%%Total pixel of detected vessels
```

```
V_d=0;
```

```
for i=1:H
```

```
    for j=1:W
```

```
        if bw_d(i,j) ==1;
```

```
            V_d = V_d+1;
```

```
        end
```

```
    end
```

```

end
V_d;

%%True positives
V_t =0;
for i=1:H
    for j=1:W
        if bw_d(i,j) ==1 & bw_a(i,j) == 1;
            V_t = V_t+1;
        end
    end
end
V_t;

%%False positives
V_f =0;
for i=1:H
    for j=1:W
        if bw_d(i,j) ==1 & bw_a(i,j) == 0;
            V_f = V_f+1;
        end
    end
end
V_f;

TPfraction = V_t/V_d
FPfraction = V_f/V_d

%%Total of 0-valued pixel (developed algorithm,)
V_o = 0; %%total of 0-valued pixel (automatic)
for i=1:H
    for j=1:W
        if bw_d(i,j) == 0;
            V_o = V_o+1;
        end
    end
end
V_o;

%%True negatives
V_tn =0;
for i=1:H
    for j=1:W
        if bw_d(i,j) ==0 & bw_a(i,j) == 0;
            V_tn = V_tn+1;
        end
    end
end
V_tn;

%%False negatives
V_fn =0;
for i=1:H
    for j=1:W

```

```

        if bw_d(i,j) ==0 & bw_a(i,j) == 1;
            V_fn = V_fn+1;
        end
    end
end
V_fn;

TNfraction = (V_tn-Outside)/(V_o-Outside)
FNfraction = V_fn/(V_o-Outside)

SP = TNfraction/(TNfraction+FPfraction)    %%Specificity
SE = TPfraction/(TPfraction+FNfraction)    %%Sensitivity
MAA = (V_t+(V_tn-Outside))/area           %%Accuracy

output=[MAA,TPfraction,FPfraction,TNfraction,FNfraction,SP,SE];

```

## ACHIEVEMENT

**2009** – Technical paper with title “Segmentation of Retinal Vasculature in Colour Fundus Images” has been accepted for “Conference on Innovative Technologies in Intelligent Systems & Industrial Applications” organized by IEEE Student Branch at Monash University, Sunway.

**2009** – Project entitled “Segmentation of Retinal Vasculature Using Active Contour Model (Snake)” won **Gold Medal Award** for Final Year Project (FYP) Category in Engineering Design Exhibition 23 (EDX23), Universiti Teknologi PETRONAS (UTP).

**2008** – Project entitled “Segmentation of Retinal Vasculature Using Active Contour Model (Snake)” won **Silver Award** for Final Year Project (FYP) Category in Electrical & Electronic Exhibition II (ElectrEx II), Universiti Teknologi PETRONAS (UTP).